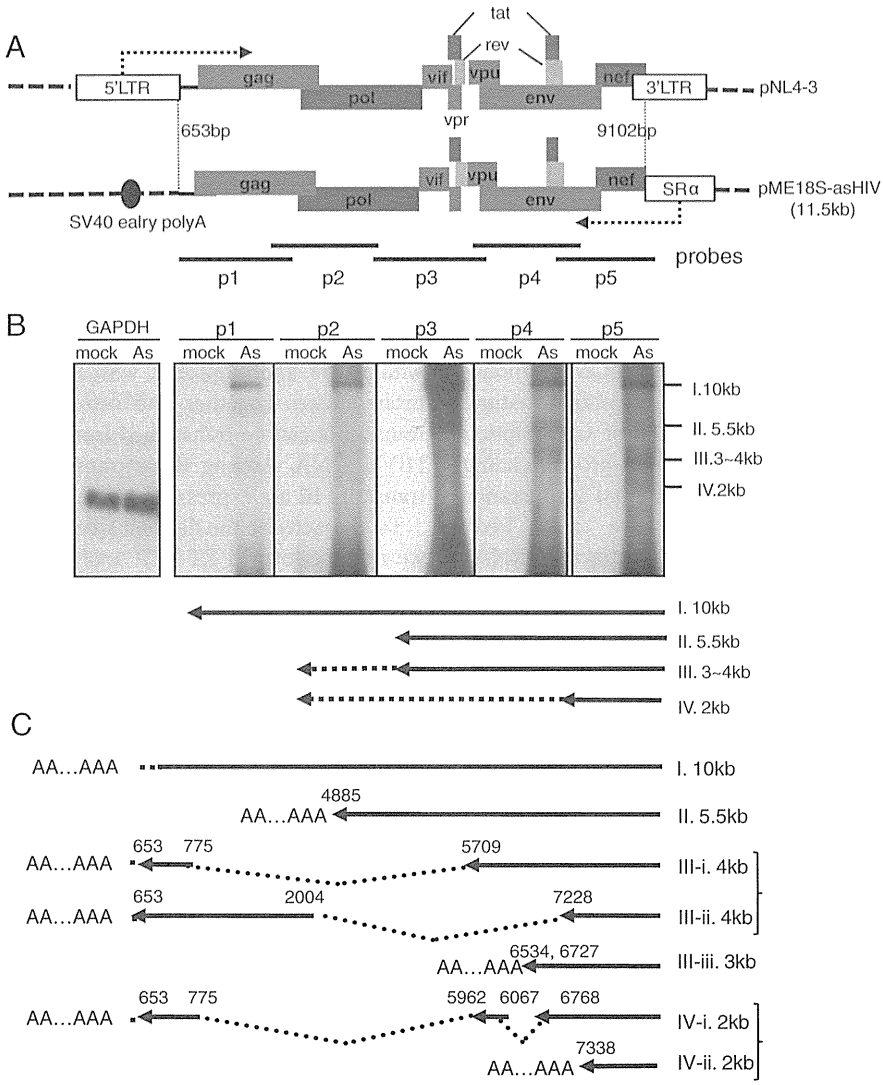

Figure 1 Mapping of the potential antisense RNAs transcribed from the HIV-1 proviral DNA. (A) A schematic diagram of the pME18S-asHIV plasmid. The antisense strand of HIV-1_{NL4-3} DNA was inserted downstream of the SRα promoter. **(B)** Results of Northern blot analysis for the detection of the RNAs from pME18S-asHIV. HEK293T cells were transfected with pME18S-asHIV or a mock vector, pME18S. Total RNA samples isolated from these cells were analyzed with region-specific probes described in A (p1–p5). *GAPDH* RNA was used as a loading control. The arrows described below are the positions of potential transcripts I–IV as described in the results. 'Mock' stands for the RNA sample extracted from cells transfected with a mock vector. 'As' stands for RNA samples extracted from cells transfected with pME18S-asHIV. **(C)** The summary of the transcription patterns in pME18S-asHIV-transfected cells. Spliced variants derived from antisense HIV-1 were identified by RT-PCR, and termination sites were determined by the 3′ RACE methods described in Additional file 1: Figure S1 and Additional file 2: Figure S2. Nucleotide numbering corresponds to the sense strand of HIV-1_{NL4-3}-DNA.

the antisense transcripts cover the region between 657 bp and 9094 bp and are unspliced forms in HIV-1 infected cells.

Identification of a novel variant of *ASP* RNA, *ASP-L*

The above results suggested that asRNAs of HIV-1, including transcripts I, II, III-iii and IV-ii, can be expressed in HIV-1-infected cells. To confirm the existence of these potential asRNAs and determine their primary structures, we next studied HIV-1 asRNAs in HIV-1-infected MAGIC-5A by 3′ RACE PCR analyses. Using the primer p4R that is located in the ASP open reading frame (ORF), a PCR product with an apparent molecular size of 700 bp was amplified in the infected MAGIC-5A cells (Figure 3A and B, lane 2 in the upper panel). In contrast to these results, no PCR products were amplified from the infected

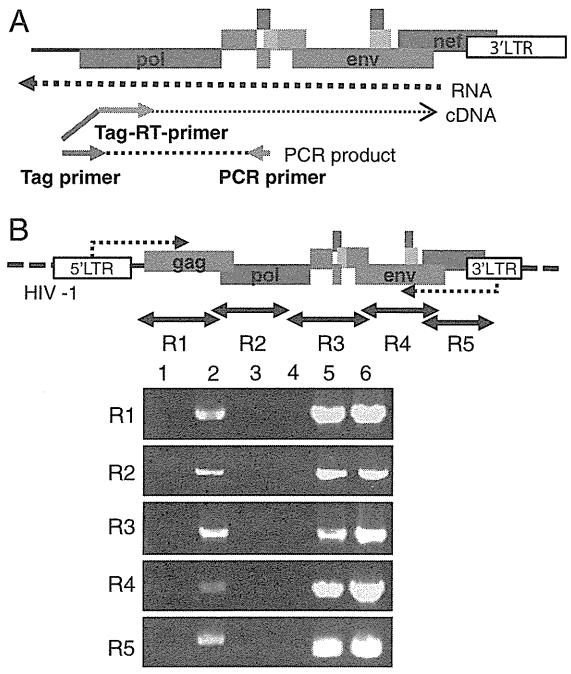

Figure 2 Antisense-specific RT-PCR of HIV-1 RNA. (A) A diagram describing the strand-specific RT-PCR method for HIV-1 asRNA. RNA samples were reverse-transcribed by an antisense-specific primer with a 5′ tag sequence (Tag-RT-primer). The synthesized cDNA samples were then amplified by PCR with a primer corresponding to the tag sequence (Tag primer) and a primer complementary to the target cDNA (PCR primer). **(B)** Detection of asRNAs in MAGIC-5A cells infected with HIV-1_{NL4-3}. The top panel describes the position of R1–R5 region. Lower panels show the results of agarose gel electrophoresis of products of the antisense-specific RT-PCR targeting R1–R5 regions. PCR products were detected corresponding to all 5 regions studied. Lane 1, MAGIC-5A without virus; Lane 2, MAGIC-5A with HIV-1_{NL4-3}; Lane 3, no RTase control; Lane 4, no RT primer control (a control for endogenous priming); Lane 5, PCR products with conventional primer pairs with cDNA samples synthesized by random primers (for testing sense and antisense RNA expressions); Lane 6, positive control (amplified from pNL4-3 plasmid DNA).

MAGIC-5A cells with the p3R primer (Figure 3B, lane 2 in the lower panel).

Semi-nested PCR using the PCR product by 3′ RACE with p4R primer produced one major product and one minor product, about 500 and 600 bp in size, in the infected MAGIC-5A cells. Analysis of the nucleotide sequences of these PCR products revealed a major poly (A) addition site that is located at the nucleotide position 6878 and other minor ones. Among the minor ones, one that extends to the nucleotide position 6783 corresponds to the larger PCR product. Thus, the results collectively showed that two groups of HIV-1 asRNAs were polyadenylated at nucleotide position 6878 (the major one) and 6783 (the minor one) in the *env* region (Figure 3C), which corresponds to the region of transcript III-iii (Figure 1C). *In silico* prediction identified a polyadenylation signal at nucleotide positions 6909 to 6918, which seems to be involved in the termination of the asRNA (Figure 3C).

Next, we studied the initiation site of the asRNA by using two reverse primers (9418r and 9538r). Antisense-specific RT-PCR with the primer 9418r successfully amplified a cDNA, whereas that with 9538r primer did not (Figure 3D). These results suggested that the transcriptional start site (TSS) is located between 9418 and 9538 of the proviral DNA. We next performed 5′ RACE to determine the TSS of the antisense transcript in the infected MAGIC-5A. The results indicated that the main TSS is at 9451 (Figure 3E), a finding supported by the successful amplification of cDNA by antisense-specific RT-PCR targeting the region between nucleotide positions of 6878 and 9451 (data not shown). *In silico* analysis predicted that this asRNA contains a few ORFs, of the previously reported *ASP* mRNA [8] and an extended 3′ UTR of approximately 500 bases compared with that of *ASP* mRNA (Figure 3A). The RT-PCR results suggested that this asRNA was mainly detected in infected MAGIC-5A cells (See Additional file 3: Figure S3).

Taken together, we have identified two new forms of asRNAs that are transcribed from the nucleotide position 9451 in the 3′ LTR U3 region of HIV DNA and terminated at nucleotide position 6878 or 6783 in the *env* region. We named these variants "*ASP* RNA-Long variant" (*ASP-L*)[GenBank: JQ866626]; a major variant terminated at 6878 is named as "*ASP-L1*," and a minor variant terminated at 6783 as "*ASP-L2*."

Transcriptional activity of the LTR in the antisense orientation

Since the transcription start sites (TSSs) of the newly characterized HIV-1 asRNAs are in the U3 region of 3′ LTR, the R-U5 region is expected to have antisense promoter activity. To study the promoter activity, we first performed a computational analysis of this region. The results revealed a potential TATA box at the nucleotide position −48 to −54 from the TSS as well as a couple of potential motifs that are recognized by transcription factors, such as CdxA, Nkx-2, and AP-1 (Figure 4A). To experimentally verify the promoter activity of this region, we performed luciferase reporter assays in Molt-4 cells using three kinds of constructs that have varying lengths of U3-R-U5 region (300 bp to140bp) in the antisense orientation (pGL4-asLTR-1, pGL4-asLTR-2, and pGL4-asLTR-3) (Figure 4A). Transfection of pGL4-asLTR-1 demonstrated a luciferase activity, the level of which was approximately one-third of that of the sense orientation LTR (pGL4-5′ LTR) (Figure 4B). Luciferase reporters having shorter regions (pGL4-asLTR-2 and pGL4-asLTR-3) also showed similar levels of promoter activities. On the other hand, a control construct that had a DNA fragment of the *env*

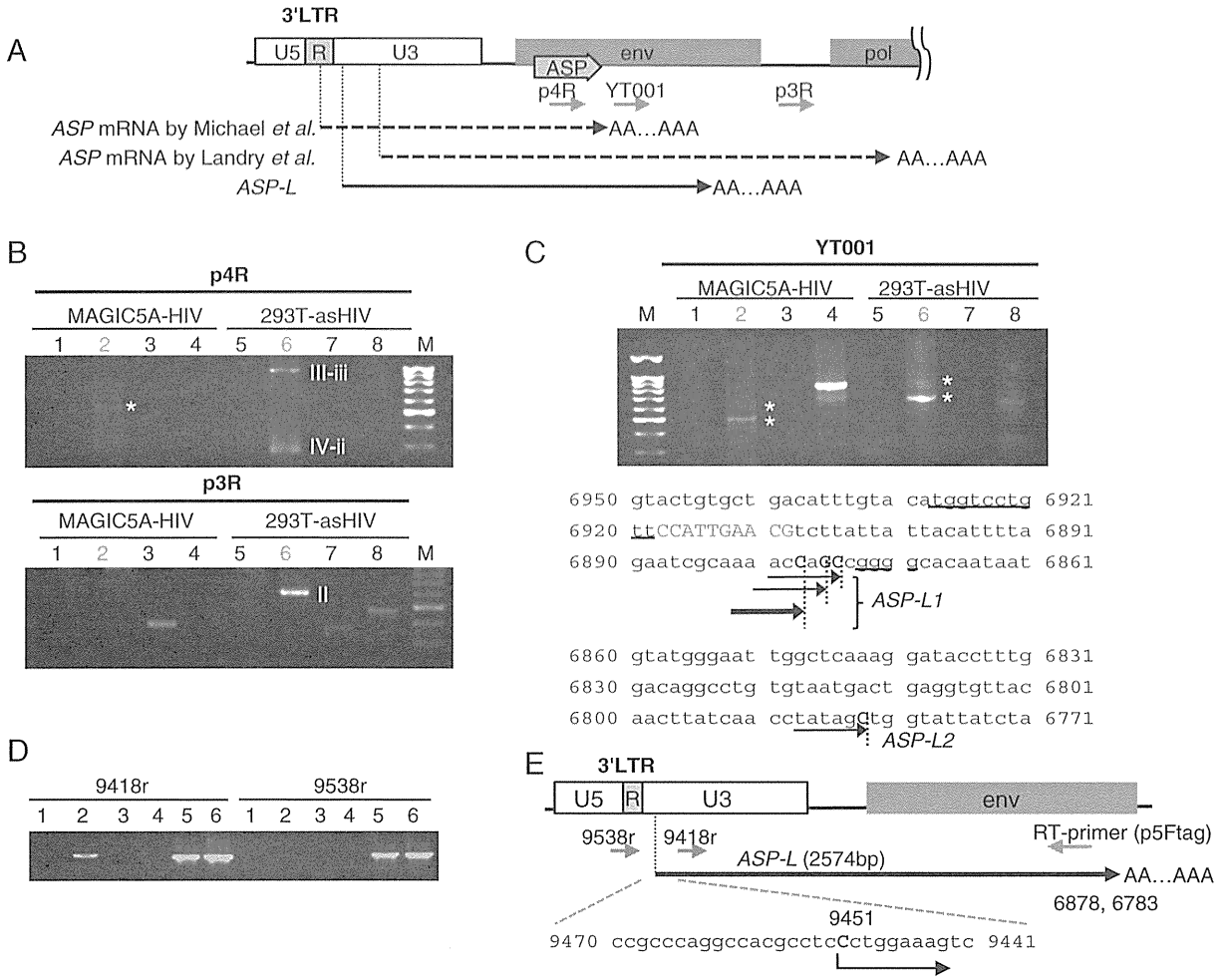

Figure 3 Identification of an antisense RNA from HIV-1-infected cells. (A) A schematic representation of the HIV-1 asRNAs and primers for 3' RACE. The black arrow represents the *ASP-L* transcript characterized in this study, and dotted arrows are the *ASP* mRNAs as previously described [8,14]. The bold green arrow indicates the position of the potential ORF, ASP. **(B and C)** Results of 3' RACE. 'MAGIC5A-HIV' stands for HIV-1 infected MAGIC-5A and '293 T-asHIV' for HEK293T cells transfected with pME18S-asHIV. Lane 1 and 5, no infection control or mock transfected cells; Lane 2 and 6, cells with HIV-1 infection or transfected with pME18S-asHIV; Lane 3 and 7, no RTase control; Lane 4 and 8, no RT-primer control; M, 100 bp marker. **(B)** The result of 3' RACE PCR using the p4R primer (upper panel) and the p3R primer (lower panel). The asterisk indicates the PCR product representing *ASP-L*. 'II', 'III-iii' and 'IV-ii' represent the PCR product derived from transcripts II, III-iii and IV-ii, respectively, described in Figure 1. **(C)** Upper panel: Results of semi-nested PCR with the YT001 primer. The white asterisks represent *ASP-L*-variant forms; the upper asterisk indicates *ASP-L2*, the lower one *ASP-L1*. The yellow asterisks represent transcript III-iii. Results of the sequencing analyses are shown in the bottom panel, where arrows and upper case letters indicate the termination sites. The bold arrow, end of the major transcript; the blue upper letters, a putative polyadenylation signal predicted by HCpolya (see Methods); the underline, putative polyadenylation elements of *ASP-L*. (D and E) Identification of transcription start site (TSS) of *ASP-L*. **(D)** Results of antisense-specific RT-PCR with two kinds of reverse primers. Locations of p5Ftag (Tag-RT-primer), 9418r, and 9538r are described in E. Lanes 1–6 are the same as in Figure 2B. **(E)** A schematic description of *ASP-L* RNA. The upper case letter C in the sequence indicates the position of *ASP-L* TSS.

region in the reverse orientation did not show any promoter activity.

To study the regulation of promoter activity of the LTR in the antisense orientation (asLTR), we next tested whether the viral accessory protein, Tat, or a cellular cytokine, TNF-α modulates the activity. Results of cotransfection experiments with a Tat expression plasmid did not show any activation of the antisense promoter, whereas the sense orientation LTR (pGL4-5′ LTR) responded to Tat in a dose-dependent manner, as expected (Figure 4C). On the other hand, TNF-α activated pGL4-asLTR-1 in a dose-dependent manner as was observed on the pGL4-5′ LTR (Figure 4D). TNF-α treatment of ACH-2 activated the expression of both strands (See Additional file 4: Figure S4).

The results shown in Figure 4D suggested the involvement of NF-κB in the regulation of 3′ LTR promoter activity in the antisense orientation. To examine this possibility, we prepared a mutant reporter (pGL4-asLTR-

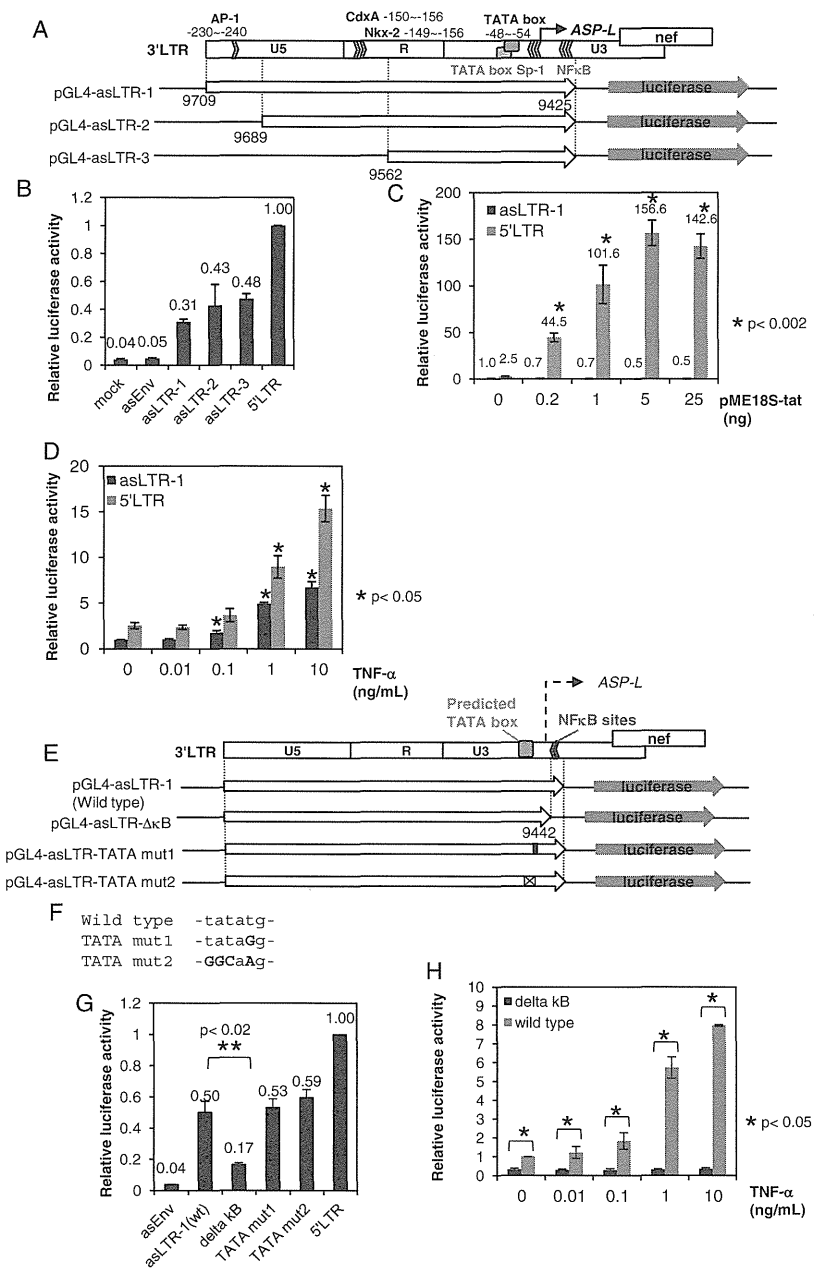

Figure 4 Transcriptional activity of the HIV-1 3' LTR in the reverse orientation. (A) A map of HIV-1 3' LTR and reporter plasmids. Top panel shows results of promoter prediction of the 5'-flanking region of the *ASP-L* TSS by TFsearch and Genetyx. Green box indicates putative TATA box. The sequence of the putative TATA box is described in F. The bottom panels are the structures of pGL4-asLTR-1, pGL4-asLTR-2 and pGL4-asLTR-3 plasmid. **(B)** Promoter activities of the LTR in the antisense orientation (asLTR). pGL4-5' LTR and pGL4-asEnv plasmids were used as positive and negative controls, respectively. mock, pGL-4.10; asEnv, pGL4-asEnv; asLTRs, pGL4-asLTR-1, pGL4-asLTR-2 and pGL4-asLTR-3; 5' LTR, pGL4-5' LTR. The luciferase activities relative to that of pGL4-5' LTR are shown. **(C)** Effects of Tat protein on the asLTR promoter activity. A Tat expression plasmid, pME18S-tat, was co-transfected with pGL4-asLTR-1 or pGL4-5' LTR. **(D)** Dose–response effects of TNF-α on the asLTR promoter activity. At 12 h post-transfection of the reporters, cells were treated with various amounts of TNF-α (0–10 ng/mL) for 12 h. **(E-H)** Investigation of transcriptional regulatory elements in the asLTR. **(E)** A schematic description of series of asLTR mutant reporters. asLTR-ΔκB lacks two NF-κB binding sites. asLTR-TATA mut1 and mut2 contain mutated TATA box. **(F)** Sequences of the potential TATA box mutants. **(G)** Promoter activities of the asLTR mutants. The luciferase activities relative to that of pGL4-5' LTR are shown. **(H)** Effects of TNF-α on the ΔκB mutant. The experimental condition is identical to D. 'delta kB' stands for pGL4-sLTR-ΔκB. 'wild type' stands for pGL4-asLTR-1. The mean ± S.D. of quadruplicate (B) or triplicate (C, D, G, and H) experiments are shown. The asterisks shown in C, D, G, and H indicate statistical significance.

ΔκB, Figure 4E), which has a deletion of NF – κB binding motifs. The basal promoter activity of the asLTR-ΔκB was significantly decreased compared with that of wild type (Figure 4G) and lost responsiveness to TNF-α treatments (Figure 4H). We further tested the possible involvement of the putative TATA box using two kinds of mutant reporters, pGL4-asLTR-TATA mut1 and pGL4-asLTR-TATA mut2 (Figure 4E and F). pGL-4asLTR-TATA mut1 has a T to G point mutation at the potential TATA box, which lacks a TATA activity [45,46]. pGL-asLTR-TATA mut2 has mutations with a deletion of the TATA motif. The results demonstrated no difference in the basal promoter activity compared with that of wild type asLTR (Figure 4G).

ASP-L expression in various types of cells infected with HIV-1

To study the expression of HIV-1 asRNAs in various types of HIV-1-infected cells, we analyzed RNA samples from Molt-4 acutely infected with HIV-1_{NL4-3}, as well as in ACH-2, and OM10.1 cell lines that are chronically infected with HIV-1_{IIIB} [47,48] with the antisense-specific RT-PCR. In this experiment, we designed an antisense-specific RT-PCR with a Tag-RT-primer that does not amplify the *ASP* mRNA reported by Michael *et al.* [8] (Figure 5A). The asRNA expression was detected in all the cell lines examined (Figure 5B). Furthermore, we could also detect asRNA in the PHA-activated PBMCs infected with HIV-1_{NL4-3} (Figure 5C). 3′ RACE analyses revealed similar transcription termination in OM10.1 and activated ACH-2 cells, where HIV-1_{IIB} also had a conserved polyadenylation signal (Figure 5D). By antisense-specific RT-PCR analyses, we demonstrated that TSS of *ASP-L* from HIV-1_{IIB} was located between nucleotide positions 9441 and 9538 that correspond with that from HIV_{NL4-3} (Figure 5E). Collectively, *ASP-L* was demonstrated to be transcribed in cell lines with acute or chronic infection as well as in primary human PBMCs infected with HIV-1.

To evaluate the expression levels of the asRNA in various cells, quantitative analysis was performed using the strand-specific quantitative RT-PCR method (qRT-PCR) of the R7 region (Figure 5A and 5F). The results showed that the highest expression level was observed in OM10.1. The expression levels of HIV-1 asRNAs were shown to be 100–2,500 times less abundant than those in the sense RNA transcripts in all cells.

Sub-cellular localization of HIV-1 antisense RNAs

The subcellular localization of asRNAs could be a key to understand the possible functions of asRNAs [30,38,49]. We, therefore, studied the localization ratios of HIV-1 asRNAs between the cytoplasm and nucleus. For this purpose, HIV-1-infected MAGIC-5A and OM10.1 cells were fractionated into the cytoplasmic and nuclear portions, followed by RNA extraction. The results of antisense strand-specific RT-PCR at R8 region revealed that the majority of HIV-1 asRNAs was enriched in the nuclear fractions in both cell lines, whereas the sense strand transcripts did not show such a biased distribution (Figure 6A). To evaluate the distribution more quantitatively, we next employed qRT-PCR at the R7 region. The results revealed that more than 77% of the asRNA is located in the nuclei of various cells including primary PHA-activated PBMC (Figure 6B–D). This significantly biased nuclear localization was also confirmed in ACH-2 and HIV-1-infected Molt-4 (See Additional file 5: Figure S5. Sub-cellular localization of HIV-1 antisense RNAs in the HIV-1 infected T cell lines). Taken together, these results indicate that *ASP* RNAs are localized mainly in the nuclei of the acutely or chronically infected cell lines as well as in the nuclei of primary PBMCs newly infected by HIV-1.

Inhibitory effects of the antisense RNA on HIV-1 replication

To understand the function of HIV-1 asRNAs, we studied the effects of *ASP-L* on HIV-1 replication. MAGIC-5A cells were transiently transfected with an *ASP-L* expression vector, pIRES-RSV-*ASP-L*, or a vacant vector, followed by infection with HIV-1. At 48 h post-transfection (p.t.), the levels of *gag* RNA decreased in *ASP-L*-expressing cells compared to those in the control cells (Figure 7A). Semi-quantitative PCR analysis of the genomic DNA did not show any significant differences in the copy numbers of the proviral DNA at p.t. 24 h, whereas it showed decreased levels of proviral DNA in *ASP-L*-expressing cells at p.t. 48 and 72 h (Figure 7B). When the virus production was evaluated by RT assays with the culture supernatants, it was decreased in the *ASP-L*-expressing cells at p.t. 72 h with statistical significance ($p < 0.002$) (Figure 7C).

To study the inhibitory effects of *ASP-L* on HIV-1 replication in T-cells, we prepared three clones of Molt-4 that stably express *ASP-L* (3C2, 3F1, and 3G9). After infecting these cells with HIV-1, viral replication was evaluated by RT assays. The results demonstrated a significant repression of viral replication in the *ASP-L*-expressing cell lines for more than 30 days post HIV-1 infection (dpi) (Figure 7D). qRT-PCR analysis of the HIV-1 sense strand RNA did not show any significant differences in the levels of *gag* and *tat* RNAs at 1 dpi between the *ASP-L*-expressing cells and mock control cells; however, it demonstrated a 5-fold reductions in the levels of *gag* and *tat* RNAs at 4 dpi in the *ASP-L*-expressing cells compared to those levels in the control cells (Figure 7E and 7F). Semi-quantitative PCR of the genomic DNA did not show a significant difference in the proviral DNA levels between *ASP-L*-expressing and control cells at 1 dpi, whereas decreased levels of proviral DNA copies were shown in *ASP-L*-expressing cells at 4 dpi (Figure 7G). Among the stable *ASP-L*-expressing cell lines, the most

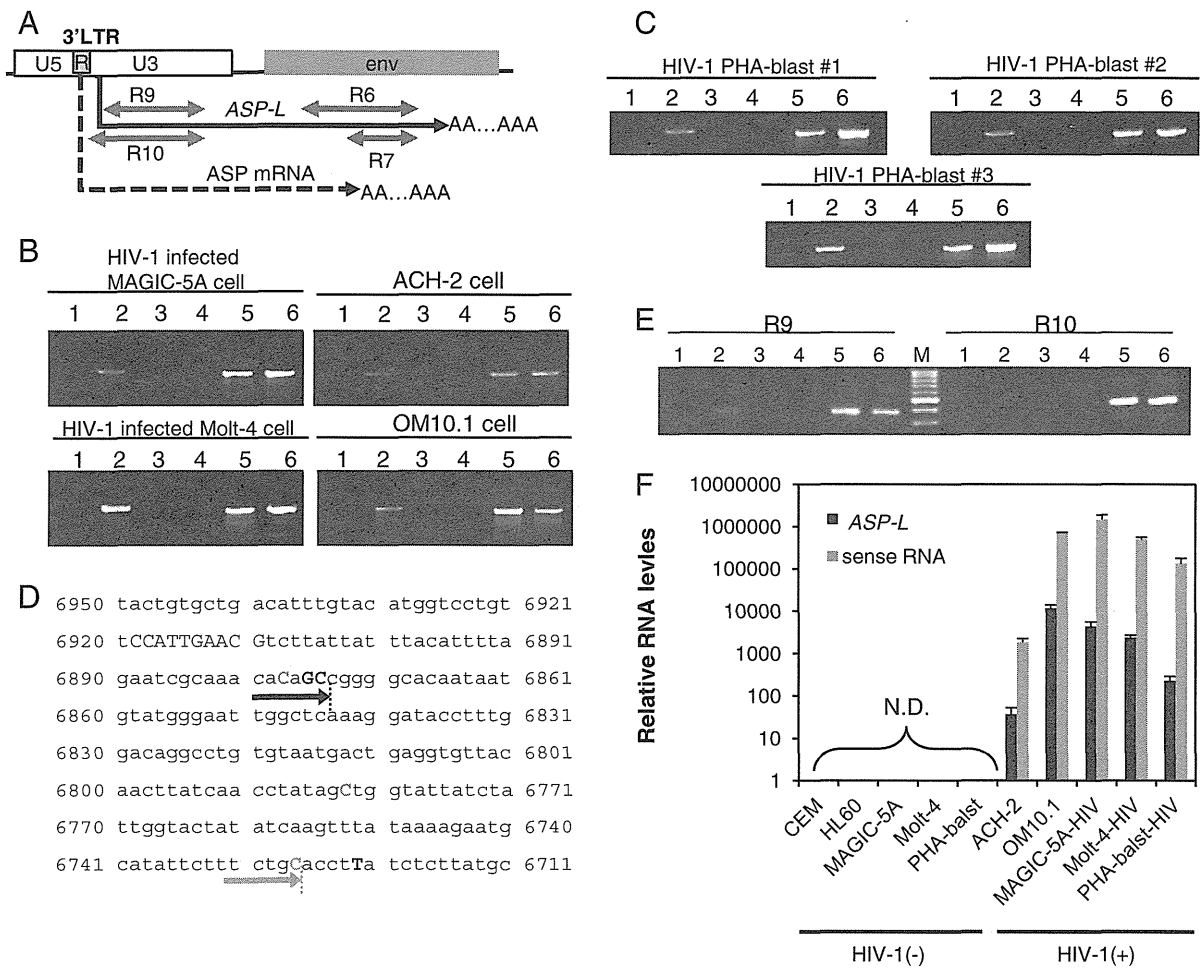

Figure 5 Expression of the HIV-1 antisense RNA in various types of HIV-1-infected cells. (A) A schematic representation of positions of *ASP-L* and *ASP* mRNA in the antisense strand of HIV-1_{NL4-3} genome. Arrows indicate the regions of the antisense-specific RT-PCR (R6, R7, R9, and R10). **(B and C)** Results of antisense-specific RT-PCR at R6 region. Total RNAs from HIV-1_{NL4-3}-newly infected Molt-4 and MAGIC-5A cells, and ACH-2 and OM10.1 chronically infected cell lines were analyzed by the antisense-specific RT-PCR **(B)**. Results of HIV-1_{NL4-3} infected-PBMCs from three healthy individuals (HIV-1-PHA-blast #1–#3) are shown in **(C)**. Lane1, uninfected cell line or PBMC; Lane 2, HIV-1 infected cell line or PBMC; Lane 3, no RTase control; Lane 4, no RT primer control, Lane 5; amplified from cDNA synthesized with random primers; Lane 6, positive control (amplified from pNL4-3 plasmid DNA or cellular genomic DNA). **(D)** Termination sites of HIV_{IIIB} *ASP-L*. Summary of 3' RACE analyses in OM10.1 and TPA-stimulated ACH-2 is shown. The upper letters mean transcription termination sites in black (ACH-2), green (OM10.1) and red (HIV-1_{NL4-3} infected MAGIC-5A cells). The black and green arrows are the major transcript in ACH-2 and OM10.1, respectively. **(E)** Determination of *ASP-L* TSS in HIV_{IIIB}. The results of antisense-specific RT-PCR at R9 and R10 are shown. Lanes 1–6 are the same as in Figure 2B. **(F)** Relative expression levels of the antisense and sense transcripts. Results of the strand-specific qRT-PCR at R7 region are shown to measure the expression levels of the antisense and sense transcripts (sense RNA). Expression levels were normalized by the levels of *β-actin* gene expression. Results of triplicated experiments are shown with mean ± S.D.

significant inhibitory effect against HIV-1 replication was observed in clone 3C2 that expresses the highest levels of *ASP-L*, where the level of *ASP-L* was estimated to be about 120 times more abundant than that in OM10.1 (Figure 7F and H). Furthermore, the nuclear localization of *ASP-L* in the *ASP-L*-expressing clones was confirmed as described above (See Additional file 6: Figure S6. Sub-cellular localization of *ASP-L* in Molt-4 stably expressing *ASP-L*). Contrary to above results, the cells expressing the 3′ region of *ASP-L* showed no inhibitory effect on HIV-1 replication (See Additional file 7: Figure S7A-C).

Upregulation of HIV-1 expression by knockdown of the endogenous antisense RNA

As described above, the enforced expression of *ASP-L* downregulated the viral gene expression and replication. We then examined the biologic effects of *ASP-L* in HIV-1 infected cells. We established Molt-4 transformants that

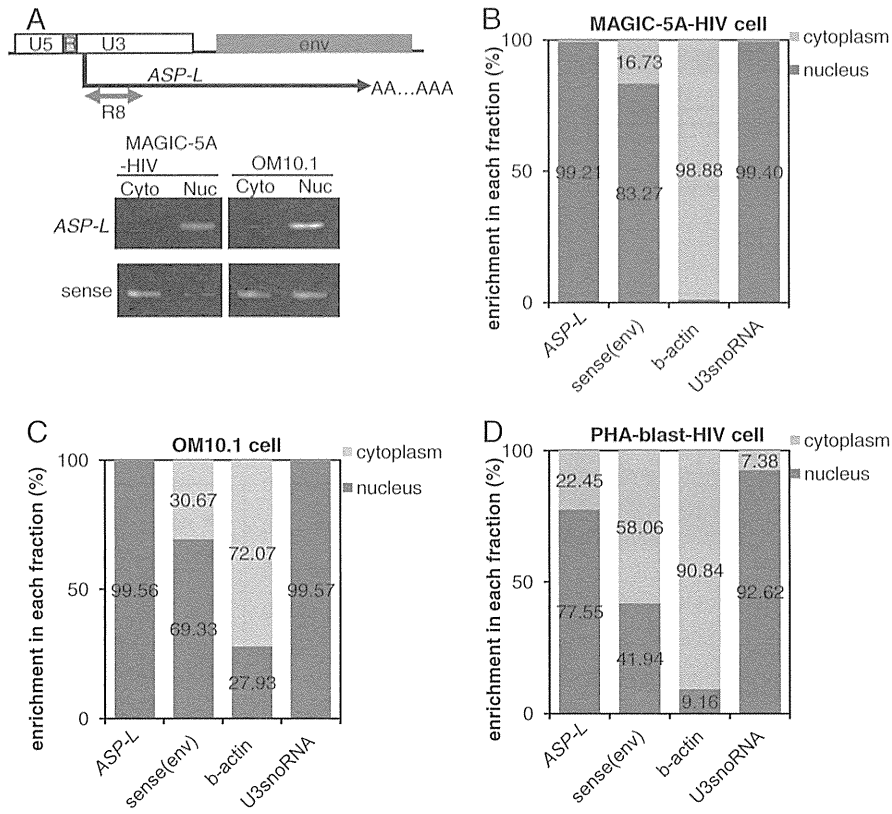

Figure 6 Sub-cellular localization of HIV-1 antisense RNAs. (A) Strand-specific RT-PCR of fractionated samples. An arrow in the upper panel indicates the region of PCR amplification (R8). Bottom panel, agarose gel electrophoresis of PCR products using samples of HIV-1-infected MAGIC-5A and chronically infected OM10.1 cells. Cyto, cytoplasmic RNA; Nuc, nuclear RNA; sense, results of sense strand-specific RT-PCR at R8. **(B–D)** Sub-cellular distribution of the asRNAs in various HIV-1-infected cells. Relative levels are presented in percentages for MAGIC-5A, OM10.1, and PHA-blast, as well as simultaneously measured controls. Results of *β-actin* cytoplasmic RNA and nuclear U3 snoRNA served as controls for fractionation efficiencies.

stably express short-hairpin RNAs (shRNAs) targeted to the HIV-1 asRNAs (shRNA#1 and shRNA#2, Figure 8A). To exclude the possible interference against sense strand RNAs, several mutated nucleotides were introduced into the passenger strands, which target to HIV-1 sense RNAs. First, we tested the specificity of these shRNAs using luciferase reporters having a sense or antisense sequence in these transformants. The two shRNAs specifically reduced the levels of luciferase activities of the reporters having *ASP-L* sequence, whereas the effects were not significant for the reporters having sense strand RNA (Figure 8B). Next, we examined the effects of these shRNAs in HIV-1 replication. The expression levels of the HIV-1 asRNAs in infected cells were suppressed in these cells compared with control cells that express a scrambled sequence (Figure 8C). qRT-PCR of RNA samples from the infected cells demonstrated significant enhancements of the levels of sense HIV-1 RNAs in the *ASP-L*-knockdown cells compared with that in the control cells (Figure 8D). Virus particle productions were evaluated by RT-assays using the supernatants of the infected cells. The RT activities were significantly enhanced in the samples of stable transformants expressing shRNA#1 and shRNA#2 compared with that of the control cells (Figure 8E).

Discussion

In the present study, to clarify the natural structure of HIV-1 asRNAs, we employed a strategy that combines an artificial overexpression of antisense strand of HIV-1 and characterization of antisense transcripts in infected cells. The results revealed a natural form of asRNAs of HIV-1_{NL4-3} and HIV-1_{IIIB}, *ASP-L*.

ASP-L appears to be a variant of previously reported *ASP* mRNA [8], in that it shares most of the region of the *ASP* mRNA, but lacks about 120 to 157 bases in the 5′ region and extends to the 3′ end by about 499 to 574 bases (Figure 3A). Previously, two groups reported structural analyses of *ASP* mRNAs (Figure 3A); first, Michael *et al.* isolated a single cDNA for *ASP* mRNA from a cDNA library prepared from A3.01 cells infected with HIV-1_{IIIB} [8]. The transcript started at the nucleotide position 9608 and polyadenylated at the nucleotide position 7367 of the HXB2

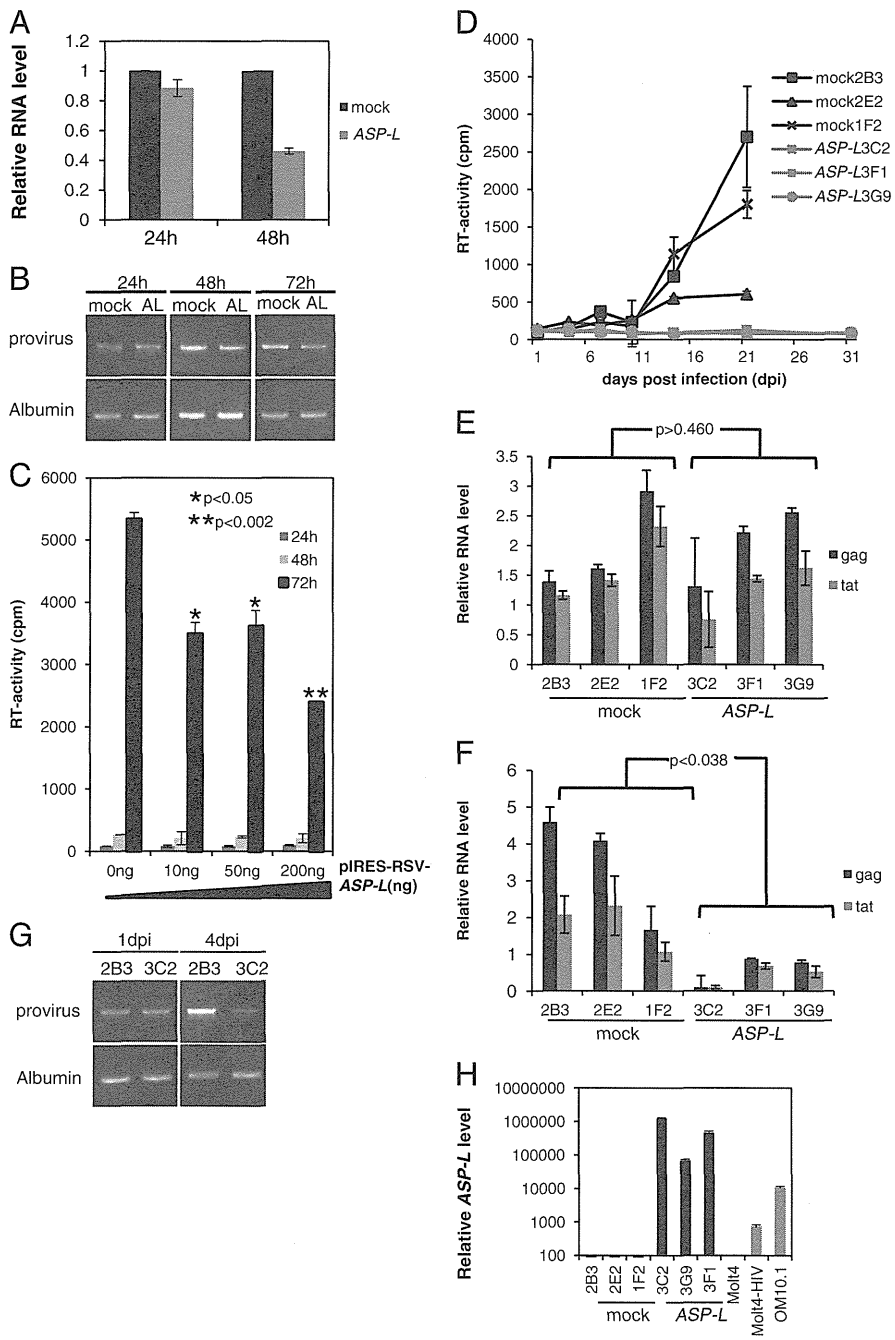

Figure 7 *ASP-L*-mediated inhibition of HIV-1 replication. Results of transient transfection experiments are shown in A to C. **(A)** HIV-1 RNA levels at the indicated time points with prior transfection of the *ASP-L* expression vector, pIRES-RSV-*ASP-L*, or a vacant vector into MAGIC-5A cells. The relative expression levels of HIV-1 *gag* RNA are presented relative to that of HIV-1 *gag* RNA expressed in mock-transfected cells set as 1.0. **(B)** Agarose gel electrophoresis of PCR products of semi-quantitative PCR of genomic DNA samples harvested at the indicated time points. 'AL' stands for pIRES-RSV-*ASP-L* transfected cells. **(C)** The levels of viral particle production in culture supernatants evaluated by RT assays. MAGIC-5A cells were transfected with the indicated amounts of the *ASP-L* expression vector before infection with HIV-1. **(D–H)** Prolonged inhibition of HIV-1 replication in *ASP-L* expressing Molt-4 clones. Three clones that stably express *ASP-L* and three clones transfected with the vacant vector were used. **(D)** The levels of virus production evaluated by RT assays. (E and F) HIV-1 RNA levels at 1 day **(E)** and 4 days **(F)** post infection (dpi) measured by qRT-PCR. **(G)** Agarose gel electrophoresis of PCR products of semi-quantitative PCR of genomic DNA samples at 1 and 4 dpi.. **(H)** The relative expression levels of *ASP-L* that were measured by qRT-PCR.

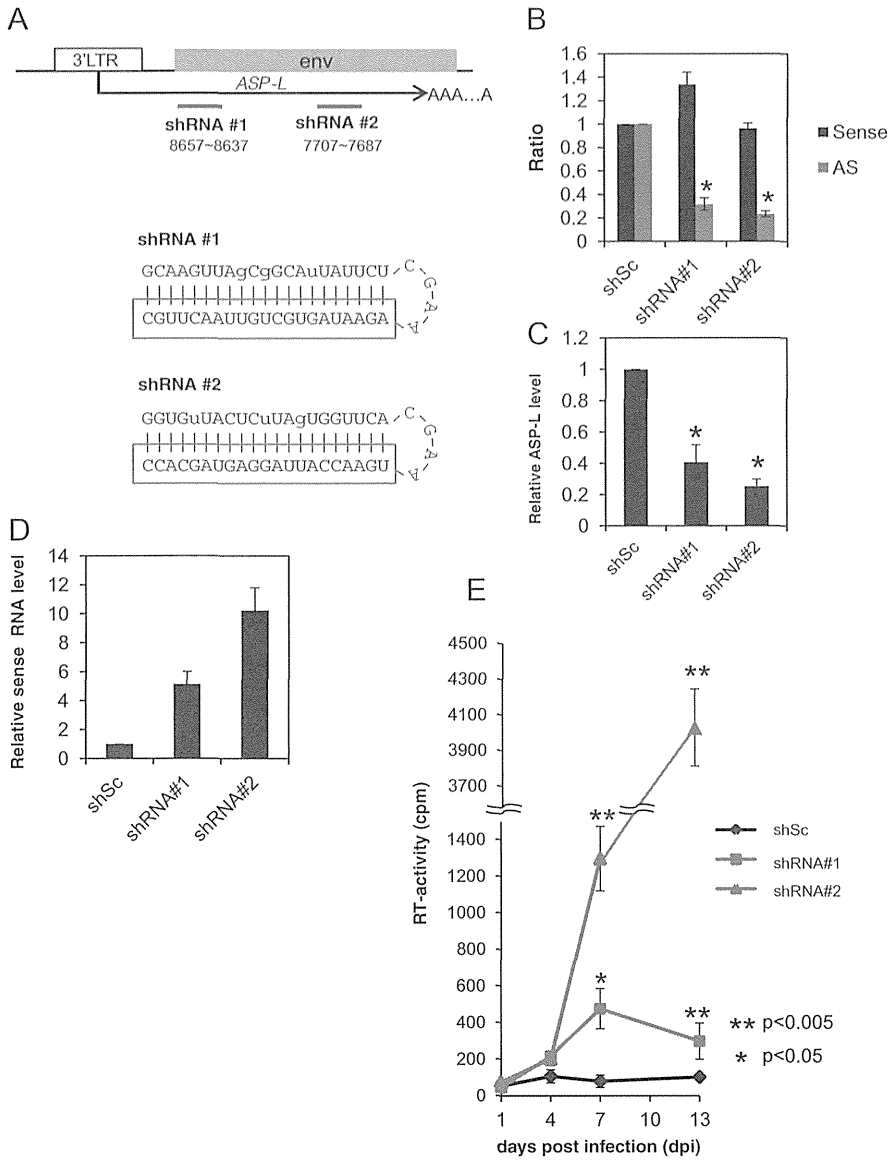

Figure 8 Effects of endogenous HIV-1 antisense RNA on HIV-1 expression. (A) Targeted regions of shRNA#1 and #2. Lower panel depicts secondary structures of expressed shRNAs predicted by m-fold. Lower case letters indicate mutated sites. Boxed sequences are guide strand for HIV-1 asRNAs. **(B)** Reporter-based confirmation of strand-specific knockdown. Luciferase reporter plasmids that contain sense HIV-1 sequence or antisense HIV-1 sequence were transfected into the shRNA-expressing Molt-4 cells. Relative changes of luciferase activities were calculated by pMIR-sense or AS *ASP-L*/pMIR-report. The mean ± S.D. of triplicate experiments are shown. Asterisks indicate statistical significance ($p < 0.01$). **(C)** Levels of endogenous HIV-1 asRNAs in HIV-1-infected shRNA expressing cells at 24 h of infection evaluated by strand-specific qRT-PCR at R7. Asterisks indicate statistical significance ($p < 0.009$). **(D)** HIV-1 sense RNA levels at 4 dpi measured by strand-specific qRT-PCR at R7 (*env* region). **(E)** Levels of viral particle production. At the indicated time points, cultured supernatant were collected and subjected to RT-assay. Asterisks indicate statistical significance.

strain, just after the TGA codon. Although a similar transcript was identified in our overexpression experiments (transcript IV-ii), this transcript was not identified in our experiments using HIV-1 infected cells (Figure 3B).

Secondly, Landry *et al.* reported the structure of another "*ASP* mRNA" in 293 T cells transfected with a 5′ LTR-deleted pNL4-3 [11]. The transcript started at various positions in the 5′ region of the 3′ LTR, and terminated in the *pol* region where they found a poly (A) signal at the nucleotide position 4908. This transcript appears to correspond to the transcript II in our overexpression experiments (Figure 1C); however, this transcript was detected only in

the 293 T cells transfected by the antisense HIV-1 expression vector, but not detected in the HIV-1 infected cells in our experiments (Figure 3B), suggesting that this form of transcripts may be an artifact in overexpression experiments. As for transcript I, the asRNAs could not be detected by 3′ RACE method; nevertheless, its expression was suggested by the antisense-specific RT-PCR in the infected MAGIC-5A (Figure 2B). These results suggested that the expression level of transcript I is lower than that of *ASP-L*.

The results of reporter assays and 5′ RACE strongly support the notion that asRNAs of HIV-1 are transcribed from 3′ LTR sequence (Figures 3 and 4). Furthermore, consistent with previous reports [8,15,50], our reporter gene assays suggested that the asRNAs of HIV-1 could be transcribed from 3′ LTR in a TATA – independent and NF-κB – dependent manner (Figure 4D-H). On the other hand, the absence of TAR sequences in the antisense transcript may explain the absence of response to Tat (Figure 4C). These results also imply a possibility that the 5′ LTR may possess a promoter activity in the antisense direction, which might contribute to modulate the expression of flanking cellular genes [6]. In addition to our findings, there remains a possibility that the antisense promoter activity may also be influenced by flanking host sequences and the action of cellular transcription factors, since HIV-1 prefers to integrate into intergenic regions of actively transcribed genes [6,51]. Also, the transcription of asRNAs might be initiated within the host flanking sequences in some cases [20].

The results of antisense-specific qRT-PCR analyses indicated that the ratio of expression levels of HIV-1 asRNAs to those of the sense transcripts varied among the cells examined (1/100 to 1/2500, Figure 5F). Our result was similar to that of a previous study in which the authors estimated 0.9% abundance of HIV-1 asRNAs to the sense transcriptions [18]. The ratio of expressions was maintained at various stages of HIV-1 infection in Molt-4 (data not shown), implying a biological meaning of *ASP-L* in a life cycle of HIV-1. Taking our data described in Figures 7 and 8 into consideration, HIV-1 might retain a balanced expression of sense and antisense genes to avoid acute toxicity. In addition, the relative expression levels of HIV-1 asRNAs compared with those of *β-actin* were confirmed to be comparable to those of mRNAs of well-known protein encoding genes with important functions such as *Bcl-2*, *Cyclin D1* and *IL-2* (data not shown).

To address the biological roles of the asRNA, we performed two experimental studies; first, using cells that stably overexpress *ASP-L*, we showed that *ASP-L* inhibits HIV-1 gene expression for a prolonged period (Figure 7). Since *ASP-L* expression did not affect the levels of HIV-1 DNA and RNA at 24 h post-transfection (Figure 7A, B, E, and G), *ASP-L* does not appear to inhibit the early processes of infection, such as viral entry and integration into the genomic DNA of target cells.

Next, we performed knockdown assays against the HIV asRNAs (Figure 8). The results suggested that asRNAs of HIV-1 including *ASP-L* might be involved in suppressing sense strand viral expression. Differences in the efficiency of viral replication between shRNA#1 and #2 may partly be attributed to their knockdown abilities (Figure 8B and C), although precise mechanisms need to be further studied. Taken collectively, the results suggest that the asRNAs may be a natural repressor for HIV-1 gene expression, which may contribute to a self-limited replication.

We demonstrated nuclear localization of *ASP-L* in the present study (Figure 6, Additional file 5: Figure S5 and Additional file 6: Figure S6). Furthermore, our data shown in Additional file 7: Figure S7 and Additional file 8 suggest that ASP protein may not be required for the antiviral function on HIV-1. These observations suggest a function of *ASP-L* that is exerted as a functional RNA. One previous study also raised a possibility that *ASP* mRNA may act as a functional RNA [13]. Recent reports demonstrated that the nuclear mRNA-like noncoding RNAs such as *Xist* and *HOTAIR* have important roles in regulating the sense strand gene expressions [39,52]. In addition, there is a possibility that *ASP-L* could be processed into small interference RNAs reducing HIV-1 replication [20].

However, considering a previous report that suggested the presence of antibodies that recognizes ASP protein in the sera of HIV-1 carriers [9], there remains a possibility that HIV asRNA may exert its functions both as a functional RNA and through protein(s) encoded by it. Considering the function of asRNA of human retroviruses, one intriguing example would be HBZ of HTLV-1. It has been reported that bZIP protein encoded by *HBZ* RNA can suppress transcription of HTLV-1 sense RNA [22,26], although antibodies that recognize HBZ have not been reported in sera of HTLV-1-infected individuals. In addition, some reports have suggested that *HBZ* RNA itself can regulate host cellular proliferation [24,25]. Further studies are required to elucidate detailed functional mechanisms of *ASP-L* and its putative translation product (s).

Conclusions

We have identified a 2.6 kb asRNA of HIV-1, a variant of *ASP* mRNAs, which is transcribed from the U3 region of antisense strand of 3′ LTR and terminates in the *env* region. The asRNA was expressed in acutely or chronically infected cells and localized in the nuclei. The expression of the asRNA led to a prolonged inhibition of HIV-1 replication, and the knockdown of the *ASP-L* RNA significantly enhanced viral replication, suggesting that HIV-1 asRNA may be a novel factor for the self-limiting replication of HIV-1. Our finding of a new regulatory asRNA of HIV-1 will improve our understanding of regulatory mechanisms

of viral replication, potentially providing a new approaches for anti-viral therapies.

Availability of supporting data

The data sets supporting the results of this article are included within the article and its additional files.

Methods

Cells and viruses

HEK293T and MAGIC-5A cells [44] were maintained in DMEM (Dulbecco's modified Eagle's medium, Nissui) supplemented with 10% of heat-inactivated fetal bovine serum (FBS, GIBCO) and antibiotics. The following cell lines were maintained with RPMI 1640 medium with 10% FBS and antibiotics: Molt-4, CEM, HL60, ACH-2 (CEM cell-derived HIV-1_{IIIB} chronically infected cell line) [47] and OM10.1 (HL-60 cell-derived HIV-1_{IIIB} chronically infected cell line) [48]. Human PBMCs were isolated from whole blood of healthy donors by Ficoll-Paque gradient centrifugation (Amersham Biosciences) and stimulated with 10 ng/mL of PHA-P (Sigma) for 48 h. The activated PBMCs (PHA-blasts) were cultured in RPMI 1640 medium supplemented with 10% FBS, antibiotics and 20 U/mL of human recombinant IL-2 (R&D systems). HIV-1 NL4-3 strain was used for the infection studies. Viral particles were produced by calcium phosphate transfection of pNL4-3 plasmid in HEK293T cells as previously described [53].

Expression vectors

Primers used for generating expression vectors are described in Additional file 9: Table S1. Primers used for this study. pME18S-asHIV was used for expression of the antisense strand of HIV-1_{NL4-3} (nucleotide position is 653 to 9102). The antisense strand of HIV-1 was obtained by PCR method with following primers: hiv-pnl-653 and hiv-pnl-9102, which are prepared based on the nucleotide sequence of pNL4-3 [53]. The PCR product was cloned into pGEM-Teasy (Promega) by TA method and subcloned into XbaI/NotI sites of pME18S [54].

The reporter gene plasmids, pGL4-asLTR-1, pGL4-asLTR-2, pGL4-asLTR-3 and pGL4-asLTR-ΔκB were generated by inserting PCR amplified fragments with varying length of the upstream sequence of *ASP-L* TSS into SacI (blunted)/XhoI sites of pGL4.10 (Promega). The fragments correspond to the following nucleotide positions of HIV-1_{NL4-3}: pGL4-asLTR-1, nucleotide position 9425 to 9709; pGL4-asLTR-2, 9425 to 9689; pGL4-asLTR-3, 9425 to 9562; pGL4-asLTR-ΔκB, 9442 to 9709. pGL4-asEnv was generated by insertion of 200 bp length antisense fragment of *env* region that was amplified by p5R and 8514f primers, followed by XbaI/XhoI digestion. pGL4–5′ LTR vector for evaluating the transcriptional activity of the sense strand LTR was described previously [55]. The TATA box mutants, pGL4-asLTR-TATA mut1 and pGL4-asLTR-TATA mut2, were prepared by site-directed gene mutagenesis method [56,57] with primers described in additional file 9. These vectors were linearized by digestion with PstI or BstXI prior to transfection. pME18S-tat was used for Tat expression [58,59].

To investigate the effect of *ASP-L* on HIV-1 replication, we prepared an *ASP-L* expression vector, pIRES-RSV-*ASP-L*, using an expression vector pIRES-RSV that was derived from pIRESpuro3 (Clontech) containing RSV promoter. pIRES-RSV-*ASP-L* was generated by inserting a proviral DNA fragment that corresponds to the full-length of *ASP-L* at EcoRI/NotI sites. The *ASP-L* fragment was obtained by PCR from pNL4-3 with primers 6878f-NotI and 9460r.

Transfections and HIV-1 infections

HEK293T cells (5×10^6) were transfected with 4 μg of plasmid DNA, pME18S-asHIV or pME18S, as a control, by Lipofectamine reagent (Invitrogen) according to the protocol of the manufacturers. After 4 h incubation, the culture medium was changed and incubated additionally for 44 h. To obtain the RNA from HIV-1-infected cells, 1.5×10^6 of MAGIC-5A cells were inoculated with HIV_{NL4-3} (3×10^3 $TCID_{50}$/50 ml) for 3 days. Total RNA was isolated by ISOGEN reagent (WAKO, Japan), followed by poly $(A)^+$ RNA selection by oligo (dT) latex (Dai-ichi Kagaku Yakuhin, Japan).

For expression of *ASP-L* gene, 200 ng of pIRES-RSV or pIRES-RSV-*ASP-L* were transfected by Lipofectamine 2000 reagent (Invitrogen). After 4 h incubation, culture medium was changed, followed by inoculation of HIV_{NL4-3} at 200 $TCID_{50}$/50 ml. After incubation for 18 h with HIV-1, cells were washed with DMEM to remove free viruses.

For establishment of T cell lines that stably express *ASP-L*, 5×10^6 of Molt-4 cells were transfected with pIRES-RSV-*ASP-L* by electroporation, and several clones were selected by 0.5 μg/mL of Puromycin (Sigma). Among the Puromycin-resistant clones, three clones were selected based on the *ASP-L* expression confirmed by RT-PCR (3C2, 3F1, and 3G9). These clones were expanded and inoculated with HIV_{NL4-3} at MOI = 0.1. After 24 h of viral attachment, cells were washed by PBS and cultured in a 6-well plate.

Northern blot analysis

Ten micrograms of total RNA samples were separated by 1% agarose-formaldehyde gel electrophoresis, and transferred onto a Biodin-A membrane (Pall). Hybridization was carried out with 7% SDS, 0.2 M Na_2HPO_4, and 1% BSA and isotope-labeled DNA probes for overnight at 65° C, followed by washing with 0.5 × SSC and 0.1% SDS at 65°C. Region specific DNA probes for p1–p5 regions were generated with PCR (See additional file 9: Table S1. Primers used for this study). The DNA fragments were TA-cloned into pGEM-Teasy vector, and the inserted DNA

was purified from SmaI/XbaI digestion of the plasmid. The probes were labeled with [α-^{32}P] dCTP by BcaBest labelling kit (TAKARA, Japan) according to the manufacture's protocol.

Strand-specific RT-PCR and quantitative RT-PCR

Primers for RT-PCR are described in the additional file 9. DNaseI-treated RNA samples were reverse-transcribed with Tag-RT-primer at 55°C for 50 min by SuperScript III reverse transcriptase (Invitrogen). Semi-quantitative RT-PCR was performed by AccuPrime DNA polymerase (Invitrogen) with the gene-specific primer and Tag primer (See also Figure 2A).

For strand-specific quantification, the cDNAs were analyzed by real-time PCR system (Thermal cycler Dice, TAKARA). The strand-specific quantitative PCR (qPCR) was performed by gene-specific primers and SYBRGreen (TAKARA). Standard curves for strand-specific qRT-PCR at R7 region were generated by linearized plasmids into which target strand-specific RT-PCR products were inserted. Levels of *b-actin* RNA were measured as internal controls [55].

3′ and 5′ RACE of antisense RNAs

Both 3′ and 5′ RACE methods were performed with 500 ng poly (A)$^+$ RNA samples according to the manufacturer's protocols (3′- and 5′-Full RACE Core Set, TAKARA). 1st and 2nd PCRs were performed by GeneTaq DNA polymerase (WAKO) with region-specific primers (See additional file 9: Table S1. primers used for this study).

In silico analyses

Genetyx ver.10 and TFsearch were utilized for the promoter analysis of the HIV-1 asRNAs. For predicting ORFs and polyadenylation signals, the sequence of *ASP-L* was analysed by ORF Finder and HCpolya.

Reporter gene assays

Linearized firefly reporter plasmid and the RSV-Renilla plasmid were co-transfected into 2×10^5 of Molt-4 cells with by Lipofectamine2000 reagent. At 24 h post-transfection, cells were harvested and evaluated the promoter activities by measurement of luciferase activities (Dual-Luciferase Reporter Assay System, Promega). Representative results of quadruplicate or triplicate experiments are presented with the mean and S.D. Treatment of TNF-α (0–10 ng/ml) was performed at 12 h post-transfection and the cells were incubated for an additional 12 h.

Sub-cellular fractionation

Cultured cells were washed with PBS and lysed with lysis buffer (10 mM Tris–HCl, pH7.5, 10 mM NaCl, 1.5 mM $MgCl_2$, 10 mM Vanadyl Complex, 1% NP-40) on ice for 5 min. After centrifugation in 3,000 rpm for 5 min at 4 C°, cytoplasmic supernatant and pelleted nuclei were separated and resuspended in ISOGEN-LS (WAKO) for RNA extraction. Relative antisense and sense strand RNA levels were measured by the strand-specific qRT-PCR method described above and calculated the enrichment of RNA levels in each compartment as below. Distribution of interested RNA was calculated as follows: (% of enrichment in each fraction) = (level of RNA in nuclear or cytoplasmic fraction)/(total levels of RNA in nuclear and cytoplasmic fractions) × 100. The efficiency of the fractionation procedure was confirmed by testing the distributions of *β-actin* cytoplasmic RNA and U3 small nucleolar RNA (U3 snoRNA) [49].

Measurement of virus production

Viral replication was evaluated by measurements of free virions in the culture media with RT assay [60]. Levels of intracellular *gag* and *tat* RNAs were measured by qRT-PCR as described previously [55]. Proviral loads were measured by PCR with p1R and p2F primers (See additional file 9: Table S1. primers used for this study) from genomic DNA samples isolated by QIAamp DNA Blood Mini Kit (Qiagen). Albumin DNA levels were used as a loading control [55].

Retroviral transduction and strand-specific RNA interference

Recombinant retroviruses carrying shRNA#1 and #2 were constructed by annealed double-strand oligonucleotides (shRNA#1, 5′-GCAAGTTAgCgGCAtTATTCTCGAAA-GAATAGTGCTGTTAACTTGC-3′; shRNA#2, 5′-GGTGtTACTCtTAgTGGTTCACGAATGAACCATTAG-GAGTAGCACC-3′) into a pSIN-sihU6 vector (TAKARA). The sequence of scrambled RNA and detailed procedure of retroviral production were as described previously [55]. After transduction of recombinant viruses and G418 selection, cells were expanded and inoculated with HIV_{NL4-3} at MOI = 0.1. After 24 hours of viral attachment, cells were washed with PBS and then cultured in a 12-well culture plate.

To confirm the strand-specific knockdown by shRNAs, the cells were transfected with pMIR-REPORT (empty plasmid, Ambion), pMIR-sense *ASP-L* or pMIR-AS *ASP-L*, respectively. These reporters include sense or antisense HIV-1 sequence in the 3′UTR of luciferase gene.

Additional files

Additional file 1: Figure S1. Determination of transcript III-iii. (A) Results of 3' RACE. Top panel summarizes the results. Agarose gel electrophoresis of 3' RACE PCR products is shown in Figure 3B. The results of the sequence analyses are shown in the bottom panel.

Bars and arrows indicate the identified termination sites. The bold arrow shows the major transcript. The upper case letters and arrows in the sequence indicate the termination sites of transcript III-iii. **(B)** Termination positions of transcript III-iii described in the context of pME18S-asHIV.

Additional file 2: Figure S2. Detection of spliced HIV-1 antisense RNAs. (A) A map of primer pairs at R11 and R12. **(B-C)** Results of agarose gel electrophoresis of antisense-specific RT-PCR products at R11 (**B**) and R12 (**C**). Expected PCR products derived from spliced transcripts were approximately 2 kb (**B**) and 400 bp (**C**), respectively (indicated by asterisks in lane 2), which are shorter than that of full-length (6 kb at R11 and 5 kb at R12). Experiments were performed using total RNAs from HEK293T with pME-18 S-asHIV (293 T-asHIV) (left panel) and HIV-1-infected MAGIC-5A (right panel). Lane 1 and 7, cells transfected with a mock vector or no infection control; Lane 2 and 8, cells with pME18S-asHIV or HIV-1 infection; Lane 3 and 9, no RTase control; Lane 4 and 10, no RT primer control; Lane 5 and 11, PCR products with conventional primer pairs with cDNA samples synthesized by random primers; Lane 6 and 12, positive control (amplified from pME18S-asHIV plasmid DNA, or from pNL4-3 plasmid DNA); M, 100 bp marker; λ, λ/Hind III marker.

Additional file 3: Figure S3. HIV-1 antisense RNA pattern in infected cells. MAGIC-5A cells were infected with HIV-1_{NL4-3} and then analyzed antisense RNAs by antisense-specific RT-PCR at regions R9 (for original *ASP* mRNA) and R10 (for *ASP-L*). Representative results (n = 4) were shown. *ASP-L* was mainly detected. Lanes 1–6 are the same as in Figure 2B.

Additional file 4: Figure S4. Transcriptional activation of HIV-1 antisense RNAs by TNF-α treatment. ACH-2 was treated with TNF-α (10 ng/mL) for 24 h. Total RNAs were extracted and analyzed by strand-specific qRT-PCR at R7. The asterisks denote statistical significance relative to the untreated control ($p < 0.02$).

Additional file 5: Figure S5. Sub-cellular localization of HIV-1 antisense RNAs in the HIV-1 infected T cell lines. Results of subcellular localization analysis of T-cell lines. RNA samples were prepared from cytoplasmic and nuclear fractions of ACH-2 cells and HIV-1_{NL4-3}-infected Molt-4 cells as described in the text.

Additional file 6: Figure S6. Sub-cellular localization of *ASP-L* in the Molt-4 cells stably expressing *ASP-L*. RNA samples were prepared from cytoplasmic and nuclear fractions of Clone 3G9 cells. Results of the quantitative measurement of RT-PCR at R7 are presented from cDNAs synthesized with random primers. Fractionation efficiencies were confirmed by measuring the levels of *β-actin* cytoplasmic RNA and nuclear U3 snoRNA.

Additional file 7: Figure S7. Inhibitory effects of full-length *ASP-L* RNA on HIV-1 replication. (A) *ASP-L* mutants. *ASP-L3'* is a portion of *ASP-L* bearing the ASP-coding region. *ASP-*$L_{\Delta ATG}$ contains an A to T mutation at the start codon of ASP. *ASP-*$L_{C\text{-}stop}$ contains a C to A mutation at the seventh codon of ASP to convert Cysteine into a stop codon. Detailed sequences are provided in the right panels. Upper cases in the nucleotide sequences show the mutated sites. **(B–C)** Effects of ASP on HIV-1 replication. **(B)** Expression levels of *ASP-L3'* measured by qRT-PCR at R7. mock, Clone 2B3 with the empty vector; wt, Clone 3C2 stably expressing wild type *ASP-L* (Figure 7D–G); c9F and c5D, established Molt-4 clones that stably express *ASP-L3'*; Molt4, uninfected Molt-4 cells; Molt4-HIV, HIV-1_{NL4-3} infected Molt-4. **(C)** HIV-1 RNA levels at 4 days post HIV-1_{NL4-3} infection. HIV-1 RNA levels were evaluated by qRT-PCR with *gag* and *tat* genes (mean ± S. D). **(D)** Effects of *ASP-L* RNA on HIV-1 replication. 50 ng or 200 ng of pIRES-RSV-*ASP-*$L_{\Delta ATG}$ (dATG) or pIRES-RSV-*ASP-*$L_{C\text{-}stop}$ (C-stop) was transfected into MAGIC-5A, followed by HIV-1_{NL4-3} infection. Viral production levels were evaluated by RT assays with the supernatants at 72 h post-transfection. **(E)** HIV-1 *gag* RNA levels at 48 h post-transfection measured by qRT-PCR.'mock' stands for MAGIC-5A with empty vector. 'wt' stands for MAGIC-5A with pIRES-RSV-*ASP-L*.

Additional file 8: Supplemental materials and methods. Supplemental materials and methods for expression vectors in Figure S7 are described.

Additional file 9: Table S1. Primers used for this study.

Abbreviations

asRNA: antisense RNA; HIV-1: Human immunodeficiency virus type 1; HTLV-1: Human T-cell leukemia virus type 1; HBZ: HTLV-1 b-ZIP protein; LTR: Long terminal repeat; PBMCs: Peripheral Blood Mononuclear Cells; PBS: Phosphate-buffered saline; PHA-P: Phytohemagglutinin-P; Tat: Trans-activator of transcription; TNF-α: Tumor necrosis factor-α.

Competing interests

The authors declare that they have no competing interests.

Acknowledgements

We gratefully appreciate for Dr. Aya Misawa, and Ms. Erica Yoshida and Mr. Tomohiro Inoue for many useful comments and help.
Grant support: Grants-in-Aid from the Ministry of Health, Labor and Welfare to TW (H19-AIDS-I-003, H22-AIDS-I-002 and H24-AIDS-008).

Author details

[1]Laboratory of Tumor Cell Biology, Department of Medical Genome Sciences, Graduate School of Frontier Sciences, The University of Tokyo, 4-6-1 Shirokanedai, Minato-ku, Tokyo 1088639, Japan. [2]Department of Microbiology, Institute of Health Biosciences, University of Tokushima Graduate School, Kuramoto-cho, Tokushima 7708503, Japan. [3]Research Center for Asian Infectious Disease, Institute of Medical Science, The University of Tokyo, 4-6-1 Shirokanedai, Minato-ku, Tokyo 1088639, Japan.

Authors' contributions

MKI improved the strand-specific RT-PCR and carried out most of the experiments and drafted the manuscript. MY advised the experimental designs and helped in drafting and finalizing the manuscripts. TH and YM helped isolate PBMC and extract cellular RNAs. RT advised the protocol used in this study and helped subcloning of shRNA-expression vectors. AM, KN, TY and TI advised the experimental design and protocols used in this study. TW conceived the study, designed the experiments and helped in drafting and finalizing the manuscripts. All authors read and approved the final manuscript.

Received: 13 May 2011 Accepted: 8 May 2012
Published: 8 May 2012

References

1. Tasara T, Hottiger MO, Hubscher U: **Functional genomics in HIV-1 virus replication: protein-protein interactions as a basis for recruiting the host cell machinery for viral propagation.** *Biol Chem* 2001, **382**(7):993–999.
2. Trkola A: **HIV-host interactions: vital to the virus and key to its inhibition.** *Curr Opin Microbiol* 2004, **7**(4):407–411.
3. Fanales-Belasio E, Raimondo M, Suligoi B, Butto S: **HIV virology and pathogenetic mechanisms of infection: a brief overview.** *Ann Ist Super Sanita* 2010, **46**(1):5–14.
4. Van Lint C, Emiliani S, Ott M, Verdin E: **Transcriptional activation and chromatin remodeling of the HIV-1 promoter in response to histone acetylation.** *EMBO J* 1996, **15**(5):1112–1120.
5. Bennasser Y, Yeung ML, Jeang KT: **HIV-1 TAR RNA subverts RNA interference in transfected cells through sequestration of TAR RNA-binding protein, TRBP.** *J Biol Chem* 2006, **281**(38):27674–27678.
6. Colin L, Van Lint C: **Molecular control of HIV-1 postintegration latency: implications for the development of new therapeutic strategies.** *Retrovirology* 2009, **6**:111.
7. Miller RH: **Human immunodeficiency virus may encode a novel protein on the genomic DNA plus strand.** *Science* 1988, **239**(4846):1420–1422.
8. Michael NL, Vahey MT, d'Arcy L, Ehrenberg PK, Mosca JD, Rappaport J, Redfield RR: **Negative-strand RNA transcripts are produced in human immunodeficiency virus type 1-infected cells and patients by a novel promoter downregulated by Tat.** *J Virol* 1994, **68**(2):979–987.
9. Vanhee-Brossollet C, Thoreau H, Serpente N, D'Auriol L, Levy JP, Vaquero C: **A natural antisense RNA derived from the HIV-1 env gene encodes a protein which is recognized by circulating antibodies of HIV + individuals.** *Virology* 1995, **206**(1):196–202.
10. Ludwig LB, Ambrus JL Jr, Krawczyk KA, Sharma S, Brooks S, Hsiao CB, Schwartz SA: **Human Immunodeficiency Virus-Type 1 LTR DNA contains an intrinsic gene producing antisense RNA and protein products.** *Retrovirology* 2006, **3**:80.
11. Landry S, Halin M, Lefort S, Audet B, Vaquero C, Mesnard JM, Barbeau B: **Detection, characterization and regulation of antisense transcripts in HIV-1.** *Retrovirology* 2007, **4**:71.

12. Peeters A, Lambert PF, Deacon NJ: **A fourth Sp1 site in the human immunodeficiency virus type 1 long terminal repeat is essential for negative-sense transcription.** *J Virol* 1996, **70**(10):6665–6672.
13. Tagieva NE, Vaquero C: **Expression of naturally occurring antisense RNA inhibits human immunodeficiency virus type 1 heterologous strain replication.** *J Gen Virol* 1997, **78**(Pt 10):2503–2511.
14. Briquet S, Vaquero C: **Immunolocalization studies of an antisense protein in HIV-1-infected cells and viral particles.** *Virology* 2002, **292(2)**:177–184.
15. Bentley K, Deacon N, Sonza S, Zeichner S, Churchill M: **Mutational analysis of the HIV-1 LTR as a promoter of negative sense transcription.** *Arch Virol* 2004, **149**(12):2277–2294.
16. Bansal A, Carlson J, Yan J, Akinsiku OT, Schaefer M, Sabbaj S, Bet A, Levy DN, Heath S, Tang J, Kaslow RA, Walker BD, Ndung'u T, Goulder PJ, Heckerman D, Hunter E, Goepfert PA: **CD8 T cell response and evolutionary pressure to HIV-1 cryptic epitopes derived from antisense transcription.** *J Exp Med* 2010, **207**(1):51–59.
17. Yeung ML, Bennasser Y, Watashi K, Le SY, Houzet L, Jeang KT: **Pyrosequencing of small non-coding RNAs in HIV-1 infected cells: evidence for the processing of a viral-cellular double-stranded RNA hybrid.** *Nucleic Acids Res* 2009, **37**(19):6575–6586.
18. Lefebvre G, Desfarges S, Uyttebroeck F, Munoz M, Beerenwinkel N, Rougemont J, Telenti A, Ciuffi A: **Analysis of HIV-1 expression level and sense of transcription by high-throughput sequencing of the infected cell.** *J Virol* 2011, **85**(13):6205–6211.
19. Clerc I, Laverdure S, Torresilla C, Landry S, Borel S, Vargas A, Arpin-Andre C, Gay B, Briant L, Gross A, Barbeau B, Mesnard JM: **Polarized expression of the membrane ASP protein derived from HIV-1 antisense transcription in T cells.** *Retrovirology* 2011, **8**:74.
20. Schopman NC, Willemsen M, Liu YP, Bradley T, van Kampen A, Baas F, Berkhout B, Haasnoot J: **Deep sequencing of virus-infected cells reveals HIV-encoded small RNAs.** *Nucleic Acids Res* 2012, **40**(1):414–427.
21. Larocca D, Chao LA, Seto MH, Brunck TK: **Human T-cell leukemia virus minus strand transcription in infected T-cells.** *Biochem Biophys Res Commun* 1989, **163**(2):1006–1013.
22. Gaudray G, Gachon F, Basbous J, Biard-Piechaczyk M, Devaux C, Mesnard JM: **The complementary strand of the human T-cell leukemia virus type 1 RNA genome encodes a bZIP transcription factor that down-regulates viral transcription.** *J Virol* 2002, **76**(24):12813–12822.
23. Cavanagh MH, Landry S, Audet B, Arpin-Andre C, Hivin P, Pare ME, Thete J, Wattel E, Marriott SJ, Mesnard JM, Barbeau B: **HTLV-I antisense transcripts initiating in the 3'LTR are alternatively spliced and polyadenylated.** *Retrovirology* 2006, **3**:15.
24. Satou Y, Yasunaga J, Yoshida M, Matsuoka M: **HTLV-I basic leucine zipper factor gene mRNA supports proliferation of adult T cell leukemia cells.** *Proc Natl Acad Sci U S A* 2006, **103**(3):720–725.
25. Arnold J, Zimmerman B, Li M, Lairmore MD, Green PL: **Human T-cell leukemia virus type-1 antisense-encoded gene, Hbz, promotes T-lymphocyte proliferation.** *Blood* 2008, **112**(9):3788–3797.
26. Matsuoka M, Green PL: **The HBZ gene, a key player in HTLV-1 pathogenesis.** *Retrovirology* 2009, **6**:71.
27. Briquet S, Richardson J, Vanhee-Brossollet C, Vaquero C: **Natural antisense transcripts are detected in different cell lines and tissues of cats infected with feline immunodeficiency virus.** *Gene* 2001, **267**(2):157–164.
28. Rasmussen MH, Ballarin-Gonzalez B, Liu J, Lassen LB, Fuchtbauer A, Fuchtbauer EM, Nielsen AL, Pedersen FS: **Antisense transcription in gammaretroviruses as a mechanism of insertional activation of host genes.** *J Virol* 2010, **84**(8):3780–3788.
29. Matsuda E, Garfinkel DJ: **Posttranslational interference of Ty1 retrotransposition by antisense RNAs.** *Proc Natl Acad Sci U S A* 2009, **106**(37):15657–15662.
30. Sasaki YT, Ideue T, Sano M, Mituyama T, Hirose T: **MENepsilon/beta noncoding RNAs are essential for structural integrity of nuclear paraspeckles.** *Proc Natl Acad Sci U S A* 2009, **106**(8):2525–2530.
31. Katayama S, Tomaru Y, Kasukawa T, Waki K, Nakanishi M, Nakamura M, Nishida H, Yap CC, Suzuki M, Kawai J, Suzuki H, Carninci P, Hayashizaki Y, Wells C, Frith M, Ravasi T, Pang KC, Hallinan J, Mattick J, Hume DA, Lipovich L, Batalov S, Engstrom PG, Mizuno Y, Faghihi MA, Sandelin A, Chalk AM, Mottagui-Tabar S, Liang Z, Lenhard B, Wahlestedt C, RIKEN Genome Exploration Research Group, Genome Science Group (Genome Network Project Core Group), FANTOM Consortium: **Antisense transcription in the mammalian transcriptome.** *Science* 2005, **309**(5740):1564–1566.
32. Wagner EG, Altuvia S, Romby P: **Antisense RNAs in bacteria and their genetic elements.** *Adv Genet* 2002, **46**:361–398.
33. Georg J, Honsel A, Voss B, Rennenberg H, Hess WR: **A long antisense RNA in plant chloroplasts.** *New Phytol* 2010, **186**(3):615–622.
34. Unver T, Bakar M, Shearman RC, Budak H: **Genome-wide profiling and analysis of Festuca arundinacea miRNAs and transcriptomes in response to foliar glyphosate application.** *Mol Genet Genomics* 2010, **283**(4):397–413.
35. Lyle R, Watanabe D, te Vruchte D, Lerchner W, Smrzka OW, Wutz A, Schageman J, Hahner L, Davies C, Barlow DP: **The imprinted antisense RNA at the Igf2r locus overlaps but does not imprint Mas1.** *Nat Genet* 2000, **25**(1):19–21.
36. Zhao J, Sun BK, Erwin JA, Song JJ, Lee JT: **Polycomb proteins targeted by a short repeat RNA to the mouse X chromosome.** *Science* 2008, **322**(5902):750–756.
37. Faghihi MA, Modarresi F, Khalil AM, Wood DE, Sahagan BG, Morgan TE, Finch CE, St Laurent G 3rd, Kenny PJ, Wahlestedt C: **Expression of a noncoding RNA is elevated in Alzheimer's disease and drives rapid feed-forward regulation of beta-secretase.** *Nat Med* 2008, **14**(7):723–730.
38. Faghihi MA, Wahlestedt C: **Regulatory roles of natural antisense transcripts.** *Nat Rev Mol Cell Biol* 2009, **10**(9):637–643.
39. Gupta RA, Shah N, Wang KC, Kim J, Horlings HM, Wong DJ, Tsai MC, Hung T, Argani P, Rinn JL, Wang Y, Brzoska P, Kong B, Li R, West RB, van de Vijver MJ, Sukumar S, Chang HY: **Long non-coding RNA HOTAIR reprograms chromatin state to promote cancer metastasis.** *Nature* 2010, **464**(7291):1071–1076.
40. Yap KL, Li S, Munoz-Cabello AM, Raguz S, Zeng L, Mujtaba S, Gil J, Walsh MJ, Zhou MM: **Molecular interplay of the noncoding RNA ANRIL and methylated histone H3 lysine 27 by polycomb CBX7 in transcriptional silencing of INK4a.** *Mol Cell* 2010, **38**(5):662–674.
41. Tufarelli C, Stanley JA, Garrick D, Sharpe JA, Ayyub H, Wood WG, Higgs DR: **Transcription of antisense RNA leading to gene silencing and methylation as a novel cause of human genetic disease.** *Nat Genet* 2003, **34**(2):157–165.
42. Luther HP: **Role of endogenous antisense RNA in cardiac gene regulation.** *J Mol Med* 2005, **83**(1):26–32.
43. Haddad F, Qin AX, Giger JM, Guo H, Baldwin KM: **Potential pitfalls in the accuracy of analysis of natural sense-antisense RNA pairs by reverse transcription-PCR.** *BMC Biotechnol* 2007, **7**:21.
44. Hachiya A, Aizawa-Matsuoka S, Tanaka M, Takahashi Y, Ida S, Gatanaga H, Hirabayashi Y, Kojima A, Tatsumi M, Oka S: **Rapid and simple phenotypic assay for drug susceptibility of human immunodeficiency virus type 1 using CCR5-expressing HeLa/CD4(+) cell clone 1–10 (MAGIC-5).** *Antimicrob Agents Chemother* 2001, **45**(2):495–501.
45. Bell SD, Brinkman AB, van der Oost J, Jackson SP: **The archaeal TFIIEalpha homologue facilitates transcription initiation by enhancing TATA-box recognition.** *EMBO Rep* 2001, **2**(2):133–138.
46. Bjornsdottir G, Myers LC: **Minimal components of the RNA polymerase II transcription apparatus determine the consensus TATA box.** *Nucleic Acids Res* 2008, **36**(9):2906–2916.
47. Folks TM, Clouse KA, Justement J, Rabson A, Duh E, Kehrl JH, Fauci AS: **Tumor necrosis factor alpha induces expression of human immunodeficiency virus in a chronically infected T-cell clone.** *Proc Natl Acad Sci U S A* 1989, **86**(7):2365–2368.
48. Butera ST, Perez VL, Wu BY, Nabel GJ, Folks TM: **Oscillation of the human immunodeficiency virus surface receptor is regulated by the state of viral activation in a CD4+ cell model of chronic infection.** *J Virol* 1991, **65**(9):4645–4653.
49. Berteaux N, Aptel N, Cathala G, Genton C, Coll J, Daccache A, Spruyt N, Hondermarck H, Dugimont T, Curgy JJ, Forne T, Adriaenssens E: **A novel H19 antisense RNA overexpressed in breast cancer contributes to paternal IGF2 expression.** *Mol Cell Biol* 2008, **28**(22):6731–6745.
50. van der Sluis RM, Pollakis G, van Gerven ML, Berkhout B, Jeeninga RE: **Latency profiles of full length HIV-1 molecular clone variants with a subtype specific promoter.** *Retrovirology* 2011, **8**:73.
51. Kilareski EM, Shah S, Nonnemacher MR, Wigdahl B: **Regulation of HIV-1 transcription in cells of the monocyte-macrophage lineage.** *Retrovirology* 2009, **6**:118.
52. Ohhata T, Hoki Y, Sasaki H, Sado T: **Crucial role of antisense transcription across the Xist promoter in Tsix-mediated Xist chromatin modification.** *Development* 2008, **135**(2):227–235.

53. Adachi A, Gendelman HE, Koenig S, Folks T, Willey R, Rabson A, Martin MA: Production of acquired immunodeficiency syndrome-associated retrovirus in human and nonhuman cells transfected with an infectious molecular clone. *J Virol* 1986, 59(2):284–291.
54. Takebe Y, Seiki M, Fujisawa J, Hoy P, Yokota K, Arai K, Yoshida M, Arai N: SR alpha promoter: an efficient and versatile mammalian cDNA expression system composed of the simian virus 40 early promoter and the R-U5 segment of human T-cell leukemia virus type 1 long terminal repeat. *Mol Cell Biol* 1988, 8(1):466–472.
55. Yamagishi M, Ishida T, Miyake A, Cooper DA, Kelleher AD, Suzuki K, Watanabe T: Retroviral delivery of promoter-targeted shRNA induces long-term silencing of HIV-1 transcription. *Microbes Infect* 2009, 11(4):500–508.
56. Barik S: Site-directed mutagenesis by double polymerase chain reaction: megaprimer method. *Methods Mol Biol* 1993, 15:277–286.
57. Yamochi T, Yamochi T, Aytac U, Sato T, Sato K, Ohnuma K, McKee KS, Morimoto C, Dang NH: Regulation of p38 phosphorylation and topoisomerase IIalpha expression in the B-cell lymphoma line Jiyoye by CD26/dipeptidyl peptidase IV is associated with enhanced in vitro and in vivo sensitivity to doxorubicin. *Cancer Res* 2005, 65(5):1973–1983.
58. Miyake A, Ishida T, Yamagishi M, Hara T, Umezawa K, Watanabe T, Horie R: Inhibition of active HIV-1 replication by NF-kappaB inhibitor DHMEQ. *Microbes Infect* 2010, 12(5):400–408.
59. Ishida T, Hamano A, Koiwa T, Watanabe T: 5' long terminal repeat (LTR)-selective methylation of latently infected HIV-1 provirus that is demethylated by reactivation signals. *Retrovirology* 2006, 3:69.
60. Willey RL, Smith DH, Lasky LA, Theodore TS, Earl PL, Moss B, Capon DJ, Martin MA: In vitro mutagenesis identifies a region within the envelope gene of the human immunodeficiency virus that is critical for infectivity. *J Virol* 1988, 62(1):139–147.

doi:10.1186/1742-4690-9-38
Cite this article as: Kobayashi-Ishihara *et al.*: HIV-1-encoded antisense RNA suppresses viral replication for a prolonged period. *Retrovirology* 2012 9:38.

Vaccine 30 (2012) 3819–3823

Contents lists available at SciVerse ScienceDirect

Vaccine

journal homepage: www.elsevier.com/locate/vaccine

Brief report

Improved neutralizing antibody response in the second season after a single dose of pandemic (H1N1) 2009 influenza vaccine in HIV-1-positive adults

Tadashi Kikuchi[a], Kiyoko Iwatsuki-Horimoto[b], Eisuke Adachi[a], Michiko Koga[a], Hitomi Nakamura[a], Noriaki Hosoya[a], Ai Kawana-Tachikawa[a], Tomohiko Koibuchi[a], Toshiyuki Miura[a,e,f], Takeshi Fujii[a], Yoshihiro Kawaoka[b,c,d], Aikichi Iwamoto[a,g,*]

[a] Division of Infectious Diseases, Advanced Clinical Research Center; Department of Infectious Disease Control, International Research Center for Infectious Diseases; and Department of Infectious Diseases and Applied Immunology, Hospital; The Institute of Medical Science, The University of Tokyo, 4-6-1 Shirokanedai, Minato-ku, Tokyo, Japan
[b] Division of Virology, Department of Microbiology and Immunology, and Department of Special Pathogens, International Research Center for Infectious Diseases, The Institute of Medical Science, The University of Tokyo, 4-6-1 Shirokanedai, Minato-ku, Tokyo, Japan
[c] ERATO Infection-Induced Host Responses Project, Japan Science and Technology Agency, 4-1-8, Honcho, Kawaguchi-shi, Saitama, Japan
[d] Department of Pathobiological Sciences, School of Veterinary Medicine, University of Wisconsin-Madison, 575 Science Drive, Madison, WI 53711, USA
[e] ViiV Healthcare K.K., 4-6-15 Sendagaya Shibuya-ku, Tokyo, Japan
[f] Institute of Tropical Medicine, Nagasaki University, 1-12-4 Sakamoto, Nagasaki, Japan
[g] Research Center for Asian Infectious Diseases, The Institute of Medical Science, The University of Tokyo, 4-6-1 Shirokanedai, Minato-ku, Tokyo, Japan

ARTICLE INFO

Article history:
Received 13 December 2011
Received in revised form 23 March 2012
Accepted 28 March 2012
Available online 10 April 2012

Keywords:
HIV
Pandemic (H1N1) 2009 influenza

ABSTRACT

Neutralizing antibody titers were determined before and after a single dose of pandemic (H1N1) 2009 influenza vaccine in HIV-1-positive Japanese adults in the first season of the pandemic and in those in the second season who had already received the vaccine in the first season. The antibody response rate at 2-month post-vaccination increased significantly from 49.0% (50/102, 95%CI: 39.0–59.1%) in the 2009/2010 season to 66.7% (42/63, 95%CI: 53.7–78.1%) in the 2010/2011 season. Geometric mean antibody titers (fold dilution) at baseline, at 2 months, and at 4 months also increased significantly from 4.4 (95%CI: 3.3–5.7), 19.0 (95%CI: 13.4–26.8) and 13.7 (95%CI: 9.3–20.2), respectively, in the 2009/2010 season to 8.3 (95%CI: 5.8–11.7), 47.0 (95%CI: 32.2–68.6) and 38.2 (95%CI: 23.8–61.4), respectively, in the 2010/2011 season. Although the vaccine response was low in the first season, it was improved in the second season.

1. Introduction

An (H1N1) influenza virus of swine origin emerged in the spring of 2009 and was transmitted rapidly, reaching pandemic levels in June 2009 [1]. The antigenic properties of the pandemic (H1N1) 2009 virus were substantially different from those of seasonal H1N1 viruses. Although the overall case fatality rate was low, this newly emerged virus caused serious illness in substantial numbers of people. Risk factors for severe illness included age < 5 years, pregnancy, chronic cardiovascular condition, chronic renal disease, chronic hepatic disease, diabetes, immunosuppression, obesity, and age ≥ 65 years, among others [2].

The World Health Organization recommended A/California/7/2009 (H1N1)-like virus as a vaccine strain on March 26th, 2009. The limited number of vaccine doses and the likelihood of increased morbidity in high-risk individuals led the Japanese Ministry of Health, Labor and Welfare Japan (MHLW) to discuss inoculation frequency and prioritized immunization schedule. Final MHLW recommendations were for a single vaccination for healthy adults, pregnant women, and high-risk individuals. HIV-1 infection was included as one of the risk factors for the prioritized immunization that started in Japan in November 2009.

Many studies have evaluated the immunogenicity of pandemic (H1N1) 2009 vaccine in HIV-1-infected populations [3–15], whose cellular and humoral immune functions may still be hampered even after initiation of antiretroviral therapy (ART) [16]. Some studies reported low rates of seroconversion (39–69% in 3 or 4 weeks post-vaccination) after pandemic (H1N1) 2009 vaccine in an HIV-1-infected population [3–10], while other studies gave inconsistent results concerning vaccine immunogenicity [11–15]. There have been few reports from Asia [6,7]. Some of the studies evaluated antibody responses after two doses of pandemic (H1N1) 2009 vaccination in the 2009/2010 season and showed improved vaccine response after the second vaccination [9,13,15,17]. Thus, results of earlier single and two-dose vaccination studies suggest that greater

* Corresponding author at: Division of Infectious Diseases, Advanced Clinical Research Center, The Institute of Medical Science, The University of Tokyo, 4-6-1 Sirokanedai, Minato-ku, Tokyo 108-8639, Japan. Tel.: +81 3 5449 5359; fax: +81 3 6409 2008.
E-mail address: aikichi@ra3.so-net.ne.jp (A. Iwamoto).

0264-410X/$ – see front matter © 2012 Elsevier Ltd. All rights reserved.
http://dx.doi.org/10.1016/j.vaccine.2012.03.083

antibody responses may be anticipated after single-dose vaccination in the second season [3–15], but there has been no report describing vaccine responses in HIV-1-infected adults in the first season of pandemic influenza compared to the second season.

We conducted a 2-year study to investigate pandemic (H1N1) 2009 vaccine responses in an HIV-1-positive population in Japan. We examined neutralizing antibody (NT) responses in two consecutive seasons following a single dose of vaccine in order to evaluate primary and secondary vaccine responses to pandemic (H1N1) 2009 in HIV-1-positive Japanese patients.

2. Methods

2.1. Patients and study design

The goal of the study was to evaluate NT responses in HIV-1-positive patients to the pandemic (H1N1) 2009 vaccine. We conducted a two-timepoint (first season and second season), cross-sectional study. In accordance with MHLW recommendations the pandemic (H1N1) 2009 vaccine was made available to HIV-1-positive Japanese adults in the outpatient clinic of the Hospital affiliated with the Institute of Medical Science, the University of Tokyo (IMSUT). The major immunization periods were from November to January in the first season (2009/2010) and from October to December in the second season (2010/2011). In the first season, HIV-1-positive patients who received the pandemic (H1N1) 2009 vaccine at our clinic were asked to participate in the study. In the second season (2010/2011), three types of vaccines were present in our clinic: those who had received their pandemic (H1N1) 2009 vaccines in both seasons at our clinic; those who had received the vaccine elsewhere in the first season (2009/2010); and those who received their first pandemic (H1N1) 2009 vaccine in the second season (2010/2011) at our clinic. We chose patients who had received the vaccines in both seasons at our clinic for analysis of the second season. For the convenience of the patients (and to increase compliance), the study visits were scheduled to coincide with routine clinic visits, which typically occur every two months.

Demographic information of the participants and relevant medical history, including ART status, were obtained from patient charts. Study procedures consisted of collection of blood samples on the day of vaccination (baseline) and at 2 months (56 ± 7 days) and 4 months (119 ± 14 days) after vaccination for assessment of (i) CD4 T-cell count and HIV-1 viral load (baseline only) and (ii) NT titers. The study was approved by the institutional ethical committee of the University of Tokyo (21-48-0108) and all study participants gave written informed consent.

2.2. Vaccine

A 0.5 mL dose of inactivated, unadjuvanted, influenza vaccine, containing 15 μg hemagglutinin of influenza virus strain A/California/7/2009 (H1N1), was used for a single intramuscular or subcutaneous vaccination in both seasons. In the 2009/2010 season the pandemic (H1N1) 2009 vaccines approved in Japan were monovalent, and we used monovalent influenza HA vaccine A (H1N1) "KAKETSUKEN" (Kaketsuken, Kumamoto, Japan). Some of the participants in the 2009/2010 season had received the seasonal trivalent vaccine (A/Brisbane/59/2007 H1N1, A/Uruguay/716/2007 H3N2, and B/Brisbane/60/2008) before or together with the pandemic (H1N1) 2009 vaccination at their own request. In the 2010/2011 season, although the same A/California/7/2009(H1N1) strain was used for manufacturing, the vaccines were trivalent with A/Victoria/210/2009 (H3N2) and B/Brisbane/60/2008 vaccines. We used the trivalent influenza HA vaccine "KAKETSUKEN" TF (Kaketsuken) in the 2010/2011 season.

2.3. Microneutrazation assay

The microneutralization assay was performed following the "WHO Manual on Animal Influenza Diagnosis and Surveillance" [18] with minor modifications as described previously [19]. We used A/Osaka/364/09 (H1N1) strain, which is antigenically very similar to A/California/7/2009 (H1N1). When the fold-dilution was below the level of detection (<1:4), the titer was designated as "1:2" for comparisons.

2.4. Data analysis

A positive NT response was defined as a 4-fold or higher increase in NT titer at 2 months post-vaccination. Geometric mean NT titers (GMT) were calculated at baseline and at 2- and 4-month post-vaccination using GraphPad Prism 5 (GraphPad Software, Inc). Changes in antibody titer were analyzed using Mann-Whitney U test, and differences in proportions of vaccine response were analyzed by the Fisher's exact test.

Multiple logistic regression analysis was performed (using JMP 9 software; SAS Institute Inc.) with the following independent variables linked to vaccine response: baseline NT titer, second season or first season, age, baseline CD4+ cell count, $\log_{10}$ HIV-1 viral load, nadir CD4+ cell count, and presence/absence of ART.

3. Results

3.1. Baseline characteristics

Two hundred thirty-one of 388 HIV-1-positive patients who visited our outpatient clinic during the immunization period in the 2009/2010 season received the vaccination, and 159 of the vaccinees agreed to participate in the study. In the 2010/2011 season, 237 of 455 HIV-1-positive patients who visited the clinic during the immunization period received the vaccination, and 186 agreed to participate. Among those 186 individuals, 116 had received the vaccine the previous year and were included in this study. Fifty-six subjects in the 2009/2010 season and 52 subjects in the 2010/2011 season failed to provide blood samples at the necessary intervals and were considered study withdrawals. The remaining population of 103 vaccinees in the 2009/2010 season and 64 vaccinees in the 2010/2011 season included 44 individuals who had participated in both seasons. One of those 44 participants was excluded from analysis because of a confirmed positive influenza A antigen test from nasopharyngeal swab in December 2009. Thus, the study populations for data analysis consisted of 102 subjects in the 2009/2010 season and 63 subjects in the 2010/2011 season.

As shown in Table 1, baseline characteristics of both groups were similar except for plasma HIV-1 viral load and proportion of subjects on ART. In the 2009/2010 season there was a lower percentage of subjects with plasma HIV-1 viral load <400 c/mL and a lower percentage of subjects on ART compared to the 2010/2011 season.

Sixty-six participants (among 102 evaluated participants) in the 2009/2010 season received the seasonal trivalent vaccine in the same season before immunization with the pandemic (H1N1) 2009 monovalent vaccine, and 28 participants received the seasonal trivalent vaccine together with the pandemic (H1N1) 2009 monovalent vaccine. Eight participants did not receive the seasonal trivalent vaccine in the 2009/2010 season.

3.2. Immune response

The 2-month post-vaccination response rate, measured as the percentage of subjects with a positive NT response (i.e., 4-fold or greater increase from baseline in NT titer), increased from 49.0% (50/102, 95%CI: 39.0–59.1%) in the 2009/2010 season to 66.7%

Table 1
Subject demographics at baseline.

	Median age (IQR)	No. of males (%)	Median CD4+ count (IQR)	Median nadir CD4+ count (IQR)	No. (%) with HIV-1 RNA <400 copies/mL	No. on ART (%)
Subjects in 1st year (n = 102)	42 years (35–51)	101 (99%)	445/μL (339–571)	183/μL (108–234)	84 (82.4%)	82 (80.4%)
Subjects in 2nd year (n = 63)	42 years (34–47)	60 (95%)	463/μL (349–609)	170/μL (74–237)	59 (93.7%)	59 (93.7%)
P value	0.61	0.16	0.58	0.61	0.057	0.022

Mann–Whitney's U-test or Fisher's exact test.
Abbreviations: IQR, interquartile range; ART, antiretroviral therapy.

(42/63, 95%CI: 53.7–78.1%) in 2010/2011 season (p = 0.036; Fig. 1A). As shown in Fig. 1B, geometric mean NT titers also increased significantly in the second season: baseline, 4.4 (95%CI: 3.3–5.7) in 2009/2010 vs. 8.3 (95%CI: 5.8–11.7) in 2010/2011 (p = 0.0002); at 2-month post-vaccination, 19.0 (95%CI: 13.4–26.8) in 2009/2010 to 47.0 (95%CI: 32.2–68.6) in 2010/2011 (p = 0.0008); and at 4-month post-vaccination, 13.7 (95%CI: 9.3–20.2) in 2009/2010 to 38.2 (95%CI: 23.8–61.4) in 2010/2011 (p = 0.0016).

3.3. Multiple logistic regression analysis

In multiple logistic regression analysis to assess factors affecting vaccine response, the only significant variables were lower baseline NT titer (adjusted odds ratio per 2-fold increase in NT titer: 0.81, 95%CI: 0.67–0.96, p = 0.014), reflecting the "law of initial value," and the second immunization season compared to the first immunization season (adjusted odds ratio: 2.66, 95%CI: 1.30–5.63, p = 0.0069) (Table 2). Indicators of immune status such as CD4 cell count, HIV-1 viral load, ART status, and age showed no significant association with vaccine response. These results suggest that the immune memory acquired in the first season improved the immune response in the following season.

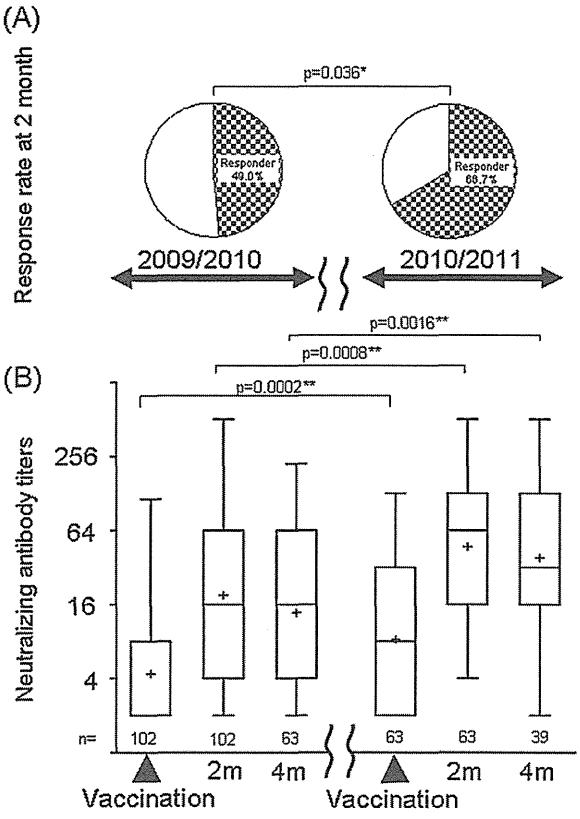

Fig. 1. Vaccine response rate (A) and geometric mean titer (B) of neutralizing antibody at 0, 2 and 4 months after vaccination in HIV-1-positive Japanese outpatients. (A) Response rate is defined by no less than 4-fold increases in neutralizing antibody (NT) titer at 2 months post vaccination compared to the baseline in each season. Subjects in 2009/2010 season were HIV-1-positive outpatients who were firstly vaccinated with single dose of non-adjuvanted pandemic (H1N1) 2009 vaccine, and subjects in 2010/2011 season were those who were secondly vaccinated with the same vaccine. (B) The 'plus' symbol represents geometric mean NT titer, horizontal line inside the box represents median NT titer, box represents inter quartile range, and whiskers represent 5–95%. *: Fisher's exact test, **: Mann–Whitney's U-test.

3.4. Influence of seasonal influenza vaccine in the 2009/2010 season

Since the pandemic (H1N1) 2009 vaccine was monovalent in the 2009/2010 season, we could classify the patients into three groups based on their history with the 2009/2010 seasonal influenza vaccine: (i) those who did not get the seasonal vaccine (non-seasonal vaccine group, n = 8), (ii) those who got both vaccines simultaneously (simultaneous seasonal vaccine group, n = 66), and (iii) those who got the seasonal vaccine before the pandemic (H1N1) 2009 vaccine (prior seasonal vaccine group, n = 28). Geometric mean baseline NT titer against pandemic (H1N1) 2009 in the 2009/2010 season was 2.6 (95%CI: 1.7–4.0), 4.3 (95%CI: 3.0–6.1) and 5.4 (95%CI: 3.1–9.4) in the three groups, respectively. Although there was a trend toward higher baseline GMT in the prior seasonal vaccine group compared to the other groups, the difference was not statistically significant (p = 0.55, Kruskal–Wallis test). Geometric mean 2-month post-vaccination NT titer against the pandemic (H1N1) 2009 was 16.0 (95%CI: 2.6–97.4), 19.7 (95%CI: 12.7–30.6) and 19.0 (95%CI: 9.5–38.0) in the non-seasonal vaccine group, the simultaneous seasonal vaccine group, and the prior seasonal vaccine group, respectively. The differences were not statistically significant (p = 0.91, Kruskal–Wallis test). The 2-month positive-vaccination response rate against the pandemic (H1N1) 2009 was 50.0% (95%CI: 15.7–84.3%) in the non-seasonal vaccine group, 53.3% (95%CI: 40.3–65.4%) in the simultaneous seasonal vaccine group and 39.3% (95%CI: 21.5–59.4%) in the prior seasonal vaccine group,. The differences were not statistically significant (p = 0.47, Chi-square test).

4. Discussion

In this two-timepoint, cross sectional study, we analyzed the neutralizing antibody response against non-adjuvanted split-virion pandemic (H1N1) 2009 vaccine in an HIV-1-positive population in two consecutive seasons. Although the positive immune response rate against pandemic (H1N1) 2009 vaccine was less than 50% in HIV-1-positive subjects in the first season of the pandemic, the rate was improved to 66.7% in the second season. We also observed a significant increase in the baseline NT titers as well as an increase in 2-month post-vaccination NT titers in the second season. Therefore, it appears that a single-dose vaccination results in a significant immune memory even after one year.

Bickel et al. [17] reported that one dose of pandemic (H1N1) 2009 vaccination in the 2009/2010 season resulted in lower

Table 2
Multiple logistic regression analysis to assess the factors associated with vaccine response.

Variable	Adjusted odds ratio	95% CI	*P* value
Season (2nd season vs 1st season)	2.66	1.30–5.63	0.0069
Baseline NT titer (per 2-fold increase)	0.81	0.67–0.96	0.014
Age (per 10-year increase)	0.76	0.54–1.05	0.097
Current CD4+ cell count (per 100/μL increase)	0.90	0.73–1.09	0.27
$\log_{10}$ HIV-1-RNA copies/mL (per 1 unit increase)	0.74	0.29–1.70	0.49
nadir CD4+ cell count (per 100/μL increase)	0.99	0.66–1.48	0.95
ART status (on ART vs not on ART)	0.39	0.03–3.88	0.43

Abbreviations: CI: confidence interval of adjusted odds ratio; ART: antiretroviral therapy; NT: neutralizing antibody.

response in a HIV-1-positive population compared to a non-HIV population but two serial doses in the same season had a booster effect and improved the response. Our study suggests that a booster effect may be expected even after a year. However, we cannot conclude that single dose in the second season is enough for HIV-1-positive patients, since 33% had insufficient response.

In our study the proportion of patients on ART was significantly higher in the second season, a difference that may have been caused by the study's design. To verify first-season vaccination, we enrolled only those subjects who had received the vaccine in our clinic. Some of the subjects who were ART-naïve when they received the first vaccine had since started ART. Many new patients are ART-naïve, but patients new to our clinic in the second season were not enrolled. Although baseline CD4+ cell counts were comparable between the two seasons, a higher ratio of the subjects on ART may have influenced the vaccine efficiency in the 2010/2011 season. However, logistic regression analysis indicated that neither ART status nor HIV-1 viral load had a significant association with vaccine response.

Our study has several limitations. First, the sample size was small and not all subjects were included in both seasons. Second, we scheduled the blood draws for the convenience of our outpatients, who are typically followed every 2 months. Consequently, NT titer assessment was done at 2 months post-vaccination, rather than at 3–4 weeks when antibody levels would be at the peak. Thirdly, we cannot rule out the influence of immune memory or antibody response from natural infection in interpreting our results, since transmission of the pandemic (H1N1) 2009 influenza via subclinical cases has been reported [20].

According to epidemiological data reported by Tokyo Metropolitan Institute of Public Health, the cumulative number of influenza-like cases per fixed surveillance point in Tokyo was 315.4 in the 2009/2010 season and 246.6 in the 2010/2011 season, and the proportion of pandemic (H1N1) 2009 influenza among the PCR-positive influenza cases was 98.6% in the 2009/2010 season and 40.8% in the 2010/2011 season [21]. Therefore, the incidence of pandemic (H1N1) 2009 influenza in Tokyo was lower in the 2010/2011 season than in the 2009/2010 season. However, as the actual rate of natural infection among the study patients was unknown, it remains a possibility that natural infection might have affected the apparent vaccine response or NT titer at baseline or 2-month post vaccination.

Finally, the difference in vaccine component, i.e., monovalent in the first season versus trivalent in the second season, might have influenced the study results. There is a possibility of cross-immunity from the Russian H1N1 strain contained in the trivalent seasonal vaccine used in the 2009/2010 season. At their request, most of our study participants in the 2009/2010 season had received the seasonal trivalent vaccine either before the pandemic (H1N1) 2009 monovalent vaccination or together with it. However, our data showed no obvious effect of seasonal influenza vaccination in the 2009/2010 season on baseline or post-vaccination NT titers of pandemic (H1N1) 2009 influenza, a finding consistent with a previous report showing that vaccination with recent seasonal nonadjuvanted or adjuvanted influenza vaccines induced little or no cross-reactive antibody response to the 2009 H1N1 influenza virus in any age group [22]. In addition, according to the regional epidemiological data, there were no cases of Russian H1N1 influenza infection detected by nasopharyngeal PCR after the emergence of pandemic (H1N1) 2009 influenza in Tokyo [21]. Therefore, it seems unlikely that our study was influenced by the seasonal (Russian) H1N1 influenza virus infection during or between the study periods.

5. Conclusion

A single dose of non-adjuvanted pandemic (H1N1) 2009 vaccine in HIV-1 positive individuals in the first season of the pandemic may improve the baseline antibody titer and the vaccine response in the second season.

Acknowledgements

This work was supported in part by a contract research fund from the Ministry of Education, Culture, Sports, Science and Technology (MEXT) for the Program of Founding Research Centers for Emerging and Reemerging Infectious Diseases and the Program of Japan Initiative for Global Research Network on Infectious Diseases; Grant-in-aid for Specially Promoted Research from MEXT; Global COE Program (Center of Education and Research for Advanced Genome-Based Medicine – for personalized medicine and the control of worldwide infectious diseases) of MEXT; Grants for Research on HIV/AIDS and Research on Publicly Essential Drugs and Medical Devises from the Ministry of Health, Labor, and Welfare of Japan (MHLW); grants-in-aid from MHLW and from ERATO (Japan Science and Technology Agency).

Potential conflicts of interest: A.I. has received speaker's honoraria from Eiken Chemical Co. Ltd., astellas, Daiichi Sankyo Co. Ltd., Toyama Chemical, Taisho Toyama Pharmaceutical Co., Ltd., Janssen Pharmaceutical K.K., Abbott Japan Co. Ltd., GlaxoSmithKline, ViiV Healthcare K.K., Bayer, Shionogi Co. Ltd., Bristol-Myers Squibb, Torii Pharmaceutical Co. Ltd., MSD, Sysmex Corporation; grant support from Toyama Chemical Co. Ltd., Torii Pharmaceutical Co. Ltd., astellas, MSD, Baxter, Bristol-Myers Squibb. Y.K. has received speaker's honoraria from Chugai Pharmaceuticals, Novartis, Daiichi-Sankyo, Toyama Chemical, Wyeth, and GlaxoSmithKline; grant support from Chugai Pharmaceuticals, Daiichi Sankyo Pharmaceutical, Toyama Chemical, Otsuka Pharmaceutical Co., Ltd.; is a consultant for Theraclone and Crucell, and is a founder of FluGen. T.K., K.I., E.A., M.K., H.N., N.H., A.K., T.K., T.M., and T.F. have no conflicts of interest.

References

[1] Itoh Y, Shinya K, Kiso M, Watanabe T, Sakoda Y, Hatta M, et al. In vitro and in vivo characterization of new swine-origin H1N1 influenza viruses. Nature 2009;460(August (7258)):1021–5.

[2] Bautista E, Chotpitayasunondh T, Gao Z, Harper SA, Shaw M, Uyeki TM, et al. Clinical aspects of pandemic 2009 influenza A (H1N1) virus infection. The New England Journal of Medicine 2010;362(May (18)):1708–19.
[3] Bickel M, Wieters I, Khaykin P, Nisius G, Haberl A, Stephan C, et al. Low rate of seroconversion after vaccination with a split virion, adjuvanted pandemic H1N1 influenza vaccine in HIV-1-infected patients. AIDS 2010;24(June (9)):F31–5.
[4] Tebas P, Frank I, Lewis M, Quinn J, Zifchak L, Thomas A, et al. Poor immunogenicity of the H1N1 2009 vaccine in well controlled HIV-infected individuals. AIDS 2010;24(September (14)):2187–92.
[5] Crum-Cianflone NF, Eberly LE, Duplessis C, Maguire J, Ganesan A, Faix D, et al. Immunogenicity of a monovalent 2009 influenza A (H1N1) vaccine in an immunocompromised population: a prospective study comparing HIV-infected adults with HIV-uninfected adults. Clinical Infectious Diseases 2011;52(January (1)):138–46.
[6] Yanagisawa N, Maeda K, Ajisawa A, Imamura A, Suganuma A, Ando M, et al. Reduced immune response to influenza A (H1N1) 2009 monovalent vaccine in HIV-infected Japanese subjects. Vaccine 2011;29(August (34)):5694–8.
[7] Hatakeyama S, Iwatsuki-Horimoto K, Okamoto K, Nukui Y, Yata N, Fujita A, et al. Unadjuvanted pandemic H1N1 influenza vaccine in HIV-1-infected adults. Vaccine 2011;29(November (49)):9224–8.
[8] Tiu CT, Lin YS, Pagala M, Ghitan M, Treanor JJ, Fitzgerald T, et al. Antibody response to inactivated influenza A (H1N1) 2009 monovalent vaccine in patients with and without HIV. Journal of Acquired Immune Deficiency Syndrome 2011;58(November (3)):e99–102.
[9] Palma P, Romiti ML, Bernardi S, Pontrelli G, Mora N, Santilli V, et al. Safety and immunogenicity of a monovalent MF59((R))-adjuvanted A/H1N1 vaccine in HIV-infected children and young adults. Biologicals 2012;(January).
[10] Fabbiani M, Di Giambenedetto S, Sali M, Farina S, Sansonetti P, Tamburrini E, et al. Immune response to influenza A (H1N1)v monovalent MF59-adjuvanted vaccine in HIV-infected patients. Vaccine 2011;29(April (16)):2836–9.
[11] Manuel O, Pascual M, Hoschler K, Giulieri S, Alves D, Ellefsen K, et al. Humoral response to the influenza A H1N1/09 monovalent AS03-adjuvanted vaccine in immunocompromised patients. Clinical Infectious Diseases 2011;52(January (2)):248–56.
[12] Kajaste-Rudnitski A, Galli L, Nozza S, Tambussi G, Di Pietro A, Pellicciotta G, et al. Induction of protective antibody response by MF59-adjuvanted 2009 pandemic A/H1N1 v influenza vaccine in HIV-1-infected individuals. AIDS 2011;25(January (2)):177–83.
[13] Launay O, Desaint C, Durier C, Loulergue P, Duval X, Jacomet C, et al. Safety and immunogenicity of a monovalent 2009 influenza A/H1N1v vaccine adjuvanted with AS03A or unadjuvanted in HIV-infected adults: a randomized, controlled trial. Journal of Infectious Diseases 2011;204(Juny (1)):124–34.
[14] Pariani E, Boschini A, Amendola A, Poletti R, Anselmi G, Begnini M, et al. Response to 2009 pandemic and seasonal influenza vaccines co-administered to HIV-infected and HIV-uninfected former drug users living in a rehabilitation community in Italy. Vaccine 2011;29(November (49)):9209–13.
[15] Soonawala D, Rimmelzwaan GF, Gelinck LB, Visser LG, Kroon FP. Response to 2009 pandemic influenza A (H1N1) vaccine in HIV-infected patients and the influence of prior seasonal influenza vaccination. PLoS ONE 2011;6(1):e16496.
[16] Cagigi A, Nilsson A, Pensieroso S, Chiodi F. Dysfunctional B-cell responses during HIV-1 infection: implication for influenza vaccination and highly active antiretroviral therapy. The Lancet Infectious Diseases 2010;10(July (7)):499–503.
[17] Bickel M, von Hentig N, Wieters I, Khaykin P, Nisius G, Haberl A, et al. Immune response after two doses of the novel split virion, adjuvanted pandemic H1N1 influenza A vaccine in HIV-1-infected patients. Clinical Infectious Diseases 2011;52(January (1)):122–7.
[18] World Health Organization. Dept. of Epidemic and Pandemic Alert and Response. WHO manual on animal influenza diagnosis and surveillance. Geneva: World Health Organization; 2002.
[19] Iwatsuki-Horimoto K, Horimoto T, Tamura D, Kiso M, Kawakami E, Hatakeyama S, et al. Seroprevalence of pandemic 2009 (H1N1) influenza A virus among schoolchildren and their parents in Tokyo, Japan. Clinical and Vaccine Immunology 2011;18(May (5)):860–6.
[20] Pang X, Yang P, Li S, Zhang L, Tian L, Li Y, et al. Pandemic (H1N1) 2009 among quarantined close contacts, Beijing, People's Republic of China. Emerging Infectious Diseases 2011 Oct;17(October (10)):1824–30.
[21] Tokyo-to Influenza Jouhou (Japanese), Tokyo Metropolitan Institute of Public Health. 2011 [cited 2012 Feb. 27]; Available from: http://idsc.tokyo-eiken.go.jp/.
[22] Hancock K, Veguilla V, Lu X, Zhong W, Butler EN, Sun H, et al. Cross-reactive antibody responses to the 2009 pandemic H1N1 influenza virus. The New England Journal of Medicine 2009;361(November (20)):1945–52.